



Chinese Pharmaceutical Association
Institute of Materia Medica, Chinese Academy of Medical Sciences

Acta Pharmaceutica Sinica B

www.elsevier.com/locate/apsb
www.sciencedirect.com



ORIGINAL ARTICLE

Discovery and druggability evaluation of pyrrolamide-type GyrB/ParE inhibitor against drug-resistant bacterial infection



Xintong Zhao[†], Jing Feng[†], Jie Zhang[†], Zunsheng Han, Yuhua Hu, Hui-Hui Shao, Tianlei Li, Jie Xia, Kangfan Lei, Weiping Wang, Fangfang Lai, Yuan Lin, Bo Liu, Kun Zhang, Chi Zhang, Qingyun Yang, Xinyu Luo, Hanyilan Zhang, Chuang Li, Wenxuan Zhang^{*}, Song Wu^{*}

State Key Laboratory of Bioactive Substance and Function of Natural Medicines, Institute of Materia Medica, Chinese Academy of Medical Sciences and Peking Union Medical College, Beijing 100050, China

Received 29 March 2023; received in revised form 7 August 2023; accepted 18 August 2023

KEY WORDS

GyrB/ParE inhibitor;
Anti-bacterial infection;
Structural modifications;
Druggability evaluation

Abstract The bacterial ATP-competitive GyrB/ParE subunits of type II topoisomerase are important anti-bacterial targets to treat super drug-resistant bacterial infections. Herein we discovered novel pyrrolamide-type GyrB/ParE inhibitors based on the structural modifications of the candidate AZD5099 that was withdrawn from the clinical trials due to safety liabilities such as mitochondrial toxicity. The hydroxyisopropyl pyridazine compound **28** had a significant inhibitory effect on Gyrase (GyrB, $IC_{50} = 49$ nmol/L) and a modest inhibitory effect on Topo IV (ParE, $IC_{50} = 1.513$ μ mol/L) of *Staphylococcus aureus*. It also had significant antibacterial activities on susceptible and resistant Gram-positive bacteria with a minimum inhibitory concentration (MIC) of less than 0.03 μ g/mL, which showed a time-dependent bactericidal effect and low frequencies of spontaneous resistance against *S. aureus*. Compound **28** had better protective effects than the positive control drugs such as DS-2969 (**5**) and AZD5099 (**6**) in mouse models of sepsis induced by methicillin-resistant *Staphylococcus aureus* (MRSA) infection. It also showed better bactericidal activities than clinically used vancomycin in the mouse thigh MRSA infection models. Moreover, compound **28** has much lower mitochondrial toxicity than AZD5099 (**6**) as well as excellent therapeutic indexes and pharmacokinetic properties. At present, compound **28** has been evaluated as a pre-clinical drug candidate for the treatment of drug-resistant

*Corresponding authors.

E-mail addresses: [wxzhang@imm.ac.cn](mailto:wzxhang@imm.ac.cn) (Wenxuan Zhang), ws@imm.ac.cn (Song Wu).

[†]These authors made equal contributions to this work.

Peer review under the responsibility of Chinese Pharmaceutical Association and Institute of Materia Medica, Chinese Academy of Medical Sciences.

<https://doi.org/10.1016/j.apsb.2023.08.030>

2211-3835 © 2023 Chinese Pharmaceutical Association and Institute of Materia Medica, Chinese Academy of Medical Sciences. Production and hosting by Elsevier B.V. This is an open access article under the CC BY-NC-ND license (<http://creativecommons.org/licenses/by-nc-nd/4.0/>).

Gram-positive bacterial infection. On the other hand, compound **28** also has good inhibitory activities against stubborn Gram-negative bacteria such as *Escherichia coli* (MIC = 1 µg/mL), which is comparable with the most potent pyrrolamide-type GyrB/ParE inhibitors reported recently. In addition, the structure–activity relationships of the compounds were also studied.

© 2023 Chinese Pharmaceutical Association and Institute of Materia Medica, Chinese Academy of Medical Sciences. Production and hosting by Elsevier B.V. This is an open access article under the CC BY-NC-ND license (<http://creativecommons.org/licenses/by-nc-nd/4.0/>).

1. Introduction

Drug-resistant bacterial infections pose a serious threat to global public health and have become one of the leading causes of human death worldwide. In 2019, approximately 1.2 million deaths were associated with bacterial resistance, and the annual number of deaths resulting from multi-drug-resistant bacterial infections is predicted to reach 10 million by 2050^{1,2}. Therefore, in addition to limiting the abuse of antibiotics and advocating the rational use of antibiotics, it is necessary to develop novel antibiotics to fight the increasingly serious infections of drug-resistant bacteria^{3,4}.

Bacterial type IIA topoisomerase can inhibit double-stranded DNA from tangling during separation and from rotation when it changes the DNA topology so that DNA replication, transcription, and recombination can proceed normally. It plays a vital role in maintaining bacterial growth and reproduction^{5,6}. Except for a few bacteria such as *Helicobacter pylori* and *Mycobacterium tuberculosis*, most bacteria express two different type IIA topoisomerases, including DNA gyrase and topoisomerase IV (Topo IV)^{7,8}.

DNA gyrase was first discovered in *Escherichia coli*. It has a GyrA₂GyrB₂ heterotetrameric structure composed of two subunits, A and B, and is mainly involved in negative supercoiling during DNA replication⁹. The subsequently discovered Topo IV has structures similar to that of gyrases. They are ParC₂ParE₂ tetramers composed of C and E subunits, which are mainly involved in the separation of progeny DNA after DNA replication. The GyrA and ParC subunits can initiate double-stranded breaks in the DNA molecule, thereby releasing the torsional tension caused by supercoiling and subsequent reconnection of the two strands. GyrB and ParE contain ATP-binding sites, and ATP hydrolysis provides the energy required for the catalytic action of GyrA and ParC^{10,11}. Blocking of the catalytic or ATP-binding sites can result in antibacterial effects, and the inhibitors are safe because the type II topoisomerase structures of eukaryotes and bacteria are different¹².

Quinolone antibiotics commonly used in clinics nowadays are DNA GyrA/ParC inhibitors, but they have certain side effects and worrisome drug resistance issues^{13,14}. By contrast, novobiocin (**1**) is the only ATP-competitive GyrB/ParE inhibitor that has ever been on the market, which was withdrawn from the market by the FDA in 2011 due to efficacy and safety issues (Fig. 1)¹⁵. The novobiocin derivative L-C43 (**2**) developed by Bristol–Myers Squibb once entered clinical trials, but its development was stopped due to side effects such as jaundice, rash, and congestive heart failure in healthy volunteers¹⁶.

With the increasingly serious problem of bacterial drug resistance in recent years, the development of antibacterial drugs targeting ATP-competitive GyrB/ParE has become a hotspot again. Many pharmaceutical companies and scientific research institutions

have begun to refocus the research and development of these targets. The rational drug design based on the X-ray structures of complexes also accelerated research progress¹⁷. At present, several GyrB/ParE inhibitors have been reported, including novobiocin derivatives, as well as synthetic pyrazoles, indazoles, arylamino-pyrimidines, pyrrolopyrimidines, pyrrolamides, imidazolamides, ethylureas, aminotricyclics and other structural classes^{18–22}. Like the novobiocin (**1**), they also have critical hydrogen bonding interactions with key amino acid Asp73 and water in the *E. coli* GyrB (Asp81 of *S. aureus* GyrB) with different groups as highlighted in red color in Fig. 1. Nevertheless, only two compounds are in clinical trials now, including SPR-720 (**4**) and DS-2969 (**5**). The ethylurea-type SPR-720 (**4**) developed by Spero Therapeutics was in phase II clinical trials for the treatment of non-tuberculous mycobacterial infections, which was the phosphate of the SPR-719 (**3**)^{23,24}. The imidazolamide-type inhibitor DS-2969 (**5**) developed by Daiichi Sankyo for the treatment of *C. difficile* infection, is currently in Phase I clinical research²⁵. It is worth noting that the above drug candidates have few inhibitory effects on most Gram-negative bacteria such as *E. coli*, similar to the vast majority of the GyrB/ParE inhibitors previously reported^{18–22}.

Besides the novobiocin and the three drug candidates in clinical trials, the pyrrolamide-type GyrB/ParE inhibitors are also attractive. The AZD5099 (**6**) developed by AstraZeneca once entered phase I clinical trials, but it was withdrawn due to safety issues^{18,26}. Although plenty of pyrrole GyrB/ParE inhibitors have been discovered by different groups since then, there was no drug candidate developed in clinical trials. Nevertheless, the efforts to find and develop pyrrolamide-type GyrB/ParE inhibitors as antibacterial drugs are continued^{18–22}. Herein, we reported the discovery of a novel pyrrolamide-type GyrB/ParE inhibitor with better antibacterial activities and druggability based on the chemical modifications of the AZD5099 (**6**).

2. Results and discussion

2.1. Design strategy

From the co-crystal complex structure with *S. aureus* GyrB (3TTZ), it can be found that the methyl dichloropyrrole carboxamide fragment of earlier AZD1279 (**7**) developed by AstraZeneca also has the critical hydrogen bonds with Asp81 (Asp73 in the *E. coli* GyrB) like other ATP-competitive GyrB/ParE inhibitors (Fig. 1)²⁷. It is noteworthy that the dichloropyrrole carboxamide moiety also existed in the natural GyrB/ParE inhibitor amycolamicin (**8**)²⁸. The substituent of a 3-*S*-methoxy group on the 4-*R*-amino-piperidine ring is also beneficial to the enzyme inhibitory activity. In addition, the thiazole interacts with Arg84 of *S. aureus* GyrB (Arg76 in *E. coli* GyrB) by cation– π stacking.

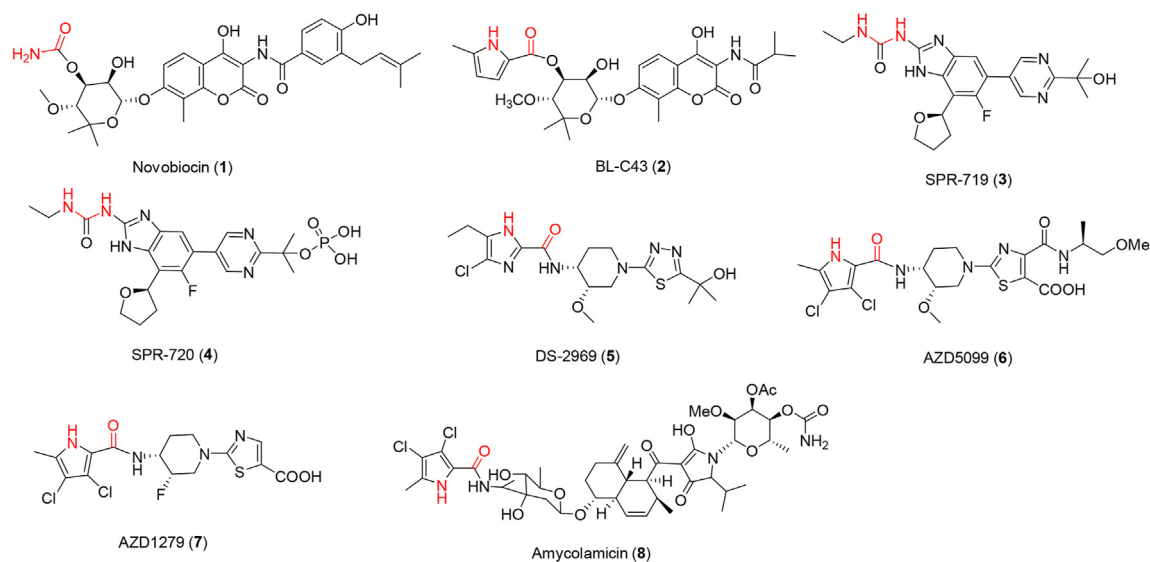


Figure 1 Representative GyrB/ParE inhibitor structure and key binding sites (in red color) for critical hydrogen bonding with GyrB/ParE subunit.

Although the carboxyl group on thiazole can generate electrostatic interaction with arginine Arg144 in *S. aureus* GyrB (Arg136 in *E. coli* GyrB) to enhance the enzyme inhibitory activity, the

AZD1279 showed moderate antibacterial activities because of the unsatisfactory cell membrane permeabilities. Moreover, the carboxyl group may lead to this compound being easily

Table 1 *In vitro* gyrase inhibitory and antibacterial activity of compounds.

Compd.	A	R ₁	Gyrase IC ₅₀ (μmol/L)		MIC (μg/mL)	
			<i>S. aureus</i>	<i>E. coli</i>	<i>S. aureus</i> (ATCC29213)	<i>E. coli</i> (ATCC25922)
9		Me	1.45 ± 0.111	>10	0.125	> 128
10		Et	0.137 ± 0.013	6.87 ± 1.221	0.125	16
11		Me	3.35 ± 0.154	>10	1	> 128
12		Me	4.87 ± 0.020	>10	0.125	> 128
13		Et	>10	>10	> 128	>128
14		Me	0.136 ± 0.020	3.12 ± 0.923	0.015	1
15		Et	>10	>10	2	> 128
16		Et	2.34	>10	0.5	128
1	/	/	0.040 ± 0.010	0.649 ± 0.227	0.5	128
5	/	/	0.376 ± 0.231	>10	0.5	64
6	/	/	0.032 ± 0.014	0.760	0.015	32

metabolized by bile anion transporters, so the *in vivo* clearance (CL) was high²⁶. After systematic structural optimization, the addition of the amide side chain on the thiazole ring can improve antibacterial activities and reduce the *in vivo* clearance, but the candidate AZD5099 (**6**) was still withdrawn from clinical trials because of mitochondrial toxicity in 2011. By contrast, the ethylurea SPR720 (**4**) and imidazolamide DS2969 (**5**) under clinical research had better safety and pharmacokinetic properties,

suggesting that replacement of the thiazole and the carboxyl group may be a promising strategy to improve the druggability of the pyrrolamide-type GyrB/ParE inhibitors.

2.1.1. The replacement of the thiazole fragment

At first, we synthesized the methyl ester of thiazole compound **9**, but the inhibitory effect against *S. aureus* gyrase was significantly reduced compared with novobiocin (**1**) and AZD5099 (**6**),

Table 2 *In vitro* gyrase inhibitory and antibacterial activity of the compounds.

II

Compd.	R ₂	Gyrase IC ₅₀ (μmol/L)		MIC (μg/mL)	
		<i>S. aureus</i>	<i>E. coli</i>	<i>S. aureus</i> (ATCC29213)	<i>E. coli</i> (ATCC25922)
17	—F	0.084 ± 0.037	8.21 ± 1.21	0.25	16
18	—Br	0.13 ± 0.017	7.42 ± 1.01	0.03	4
19	—CF ₃	0.12 ± 0.047	9.31 ± 0.923	0.03	16
20	—CN	0.701 ± 0.248	>10	0.06	> 128
21		0.825 ± 0.303	>10	0.06	> 128
22		0.045 ± 0.009	0.788 ± 0.289	0.015	1
23		1.49 ± 0.234	2.56	0.008	1
24		2.07 ± 0.568	>10	0.03	> 128
25		0.172 ± 0.056	>10	0.25	> 128
26		0.052 ± 0.013	0.869 ± 0.313	0.125	> 128
27		0.094 ± 0.040	5.11 ± 0.545	0.03	4
28		0.049 ± 0.005	1.48 ± 0.441	0.008	1
29		0.397 ± 0.024	>10	0.25	8
30		0.696 ± 0.056	>10	0.125	16
31		0.576 ± 0.045	>10	0.125	> 128
32		>10	>10	32	64
33		1.09 ± 0.146	>10	0.25	32
34		>10	>10	32	> 128
35		>10	>10	32	> 128
36		>10	>10	0.5	16

Table 3 *In vitro* gyrase inhibitory on Topo IV [IC_{50} ($\mu\text{mol/L}$)].

Strains	1	14	22	26	28
<i>S. aureus</i>	0.383 \pm 0.120	7.180 \pm 2.809	2.128 \pm 0.753	5.706 \pm 2.137	1.513 \pm 0.460
<i>E. coli</i>	\sim 10	>10	>10	>10	>10

possibly because of the loss of the original electrostatic effect between the carboxyl group and Arg144 (Table 1). Nevertheless, the thiadiazole ester **10** was more potent than compound **9** against *S. aureus* gyrase, but the antibacterial activity (MIC = 0.125 mg/mL) was not improved possibly because of the insufficient membrane permeability. The following replacements of pyridine **11**, pyrazine **12** and pyrimidine **13** led to the reduction of the activities, but the pyridazinyl **14** showed a comparable *S. aureus* gyrase inhibitory effect as compound **10**. To our delight, the pyridazine derivative **14** showed 8 folds stronger antibacterial activity against *S. aureus* strain (MIC = 0.015 $\mu\text{g/mL}$) than thiadiazole **10**, with the same MIC value as AZD5099 (**6**), possibly because of the promotion of physicochemical properties by the pyridazine. Although the oxazole derivative **16** showed better inhibitory activity than the oxadiazole compound **15**, it was less active than thiadiazole compound **10**.

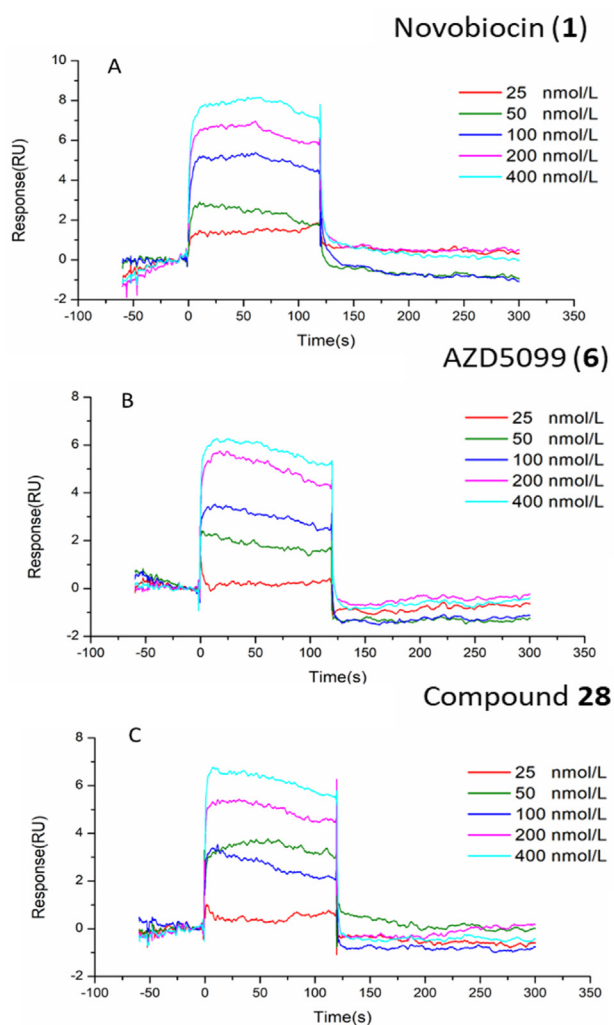
Overall, the synthesized compounds have a significantly stronger inhibitory effect on *S. aureus* gyrase than *E. coli* gyrase, which is similar to Novobiocin (**1**) and AZD5099 (**6**). Except for thiadiazole **10** and pyridazine **14**, the IC_{50} values of the other compounds against *E. coli* gyrase were larger than 10 $\mu\text{mol/L}$. Although compound **14** showed a weaker *E. coli* gyrase inhibitory effect than novobiocin (**1**) and AZD5099 (**6**), its antibacterial activity against *E. coli* was significantly improved, which is comparable to the most potent pyrrolamide-type GyrB/ParE inhibitors reported recently, indicating the compound could also penetrate impenetrable outer cell membranes of Gram-negative bacteria^{29,30}.

However, compound **14** showed a weak protective effect at 10 mg/kg by intragastric administration (ig) in a mouse model of sepsis induced by the methicillin-resistant *S. aureus* (ATCC43300) infection (Fig. 4). The poor metabolic stabilities of the methyl ester *in vivo* may be a major reason. Nevertheless, the excellent gyrase inhibitory and antibacterial activities of pyridazine **14** gave us great confidence to continue the optimization of its structure.

2.1.2. The structural optimization of substituents on the pyridazine ring

When the methyl ester group (**14**) was replaced by fluorine (**17**), bromine (**18**), or trifluoromethyl (**19**), the *S. aureus* gyrase inhibitory activities of the compounds were almost maintained, but the compound **17** with low lipophilicity was less potent in the bacterial cell (Table 2). Although the inhibitory activities of the cyano compound **20** and acetyl compound **21** were reduced, the trifluoroacetyl compound **22** showed better gyrase inhibitory activities than compound **14**. The compound **22** also showed better antibacterial activities than the other compounds, with a MIC value of 0.015 $\mu\text{g/mL}$. Compared with the oxime **23** and its methyl derivative **24**, the carboxyl oxime ether **25** and **26** have stronger inhibitory activities against *S. aureus* gyrase, possibly because the carboxyl groups have additional electrostatic interactions with the Arg144 of *S. aureus* gyrase. However, the neutral compounds **23** and **24** showed better antibacterial activities than carboxyl compounds **25** and **26**, indicating that they are easier to penetrate the cell membranes of bacteria and the oxime/methyl oxime ether may enhance the antibacterial activities in other ways.

The hydroxyalkyl compounds **27** and **28** showed slightly better gyrase inhibitory activities than compound **14**, especially compound **28** showed the best gyrase inhibitory and antibacterial activities against the *S. aureus* (IC_{50} = 49 nmol/L, MIC = 0.008 $\mu\text{g/mL}$). The amide compounds **29–31** and **33** have moderate *S. aureus* gyrase inhibitory and antibacterial activities, but the basic

**Figure 2** The affinity of the compounds with GyrB by SPR.**Table 4** The affinity of the compounds with GyrB by SPR [K_D (nmol/L)].

Strains	1	6	28
<i>S. aureus</i> GyrB24	69.6	83.8	52

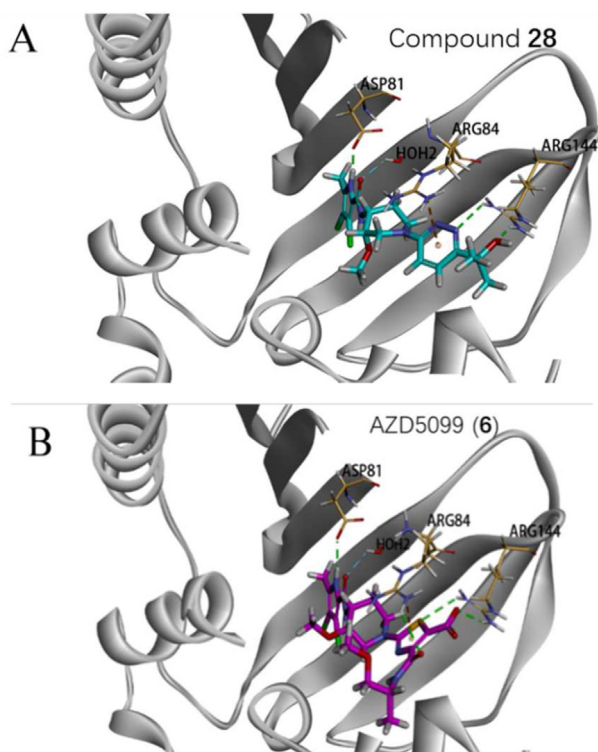


Figure 3 Molecule docking of compound **28** and AZD5099 (**6**) with *S. aureus* GyrB.

N-aminoethyl amide **32**, aminomethyl **34**, amidine **35**, and the acidic tetrazolium **36** were significantly less potent.

For the *E. coli* gyrase, the trifluoroacetyl compound **22** and carboxyl oxime ether **26** showed the best inhibitory activities with IC_{50} values less than 1 $\mu\text{mol/L}$. In addition, the neutral compounds **17–19** and **27–28** also showed moderate inhibitory activities with IC_{50} values below 10 $\mu\text{mol/L}$. The compounds **22**, **23** and **28** also showed the best antibacterial activities against the *E. coli* strain with MIC as 1 $\mu\text{g/mL}$, similar to compound **14**. By contrast, the carboxyl compound **26** was inactive, indicating that it was hindered from penetrating the outer cell membrane of the *E. coli* bacteria.

The Topo IV inhibitory activities (ParE) of representative compounds **14**, **22**, **26** and **28** were assayed subsequently with novobiocin (**1**) (Table 3). Just like novobiocin (**1**), the compounds show relatively weaker inhibitory activities on Topo IV than gyrase, with the IC_{50} values as 1.513–7.180 $\mu\text{mol/L}$ on *S. aureus* Topo IV and more than 10 $\mu\text{mol/L}$ on *E. coli* Topo IV in our ATPase assay.

2.2. Surface plasmon resonance (SPR) and molecule docking

2.2.1. SPR studies

To verify further the interaction of the compounds with the gyrase B subunit (GyrB24; residues 2–220), we performed the surface plasmon resonance (SPR) experiment with novobiocin (**1**) and AZD5099 (**6**) as positive controls (Fig. 2 and Table 4)¹⁸. As expected, compound **28** had a value for K_D in the range 10^{-8} – 10^{-9} mol/L, just like the novobiocin (**1**) and AZD5099 (**6**), indicating they bind with GyrB with high affinities.

2.2.2. Molecule docking

From the molecule docking with *S. aureus* GyrB (cocrystal with AZD1279, 3TTZ), it can be found that compound **28** has a similar interaction mode with AZD5099 (**6**) (Fig. 3). At first, both of the methyl dichloropyrrole carboxamide fragments of compound **28** and AZD5099 (**6**) formed the critical hydrogen bonds with Asp81 and water in nearly the same manner. Although the 3-methoxyl groups on the piperidine rings took different conformations, the pyridazine of compound **28** and the thiazole of AZD5099 (**6**) formed similar cation– π stacking interactions with Arg84. In addition, the nitrogen atom of the pyridazine and oxygen atom of the hydroxyisopropyl group of compound **28** formed the hydrogen-bonding interactions with Arg144, which also can be found in the sulfur atom of the thiazole and oxygen atom of the carboxyl group of the AZD5099 (**6**).

2.3. The mouse model of sepsis induced by MRSA

Using a mouse model of sepsis induced by the methicillin-resistant *S. aureus* (ATCC43300) infection, the protective effects of compounds **22**, **23** and **28** that showed comparable *in vitro* inhibitory activities against *S. aureus* ($MIC \leq 0.015$ $\mu\text{g/mL}$) were evaluated through intragastric administration (ig) at a dose of 10 mg/kg, with DS2969b (**5**) and AZD5099 (**6**) as controls (Fig. 4)³¹. The experimental results showed that compounds **22** and **23** show weak protective effects, just like the lead compound **14**. Although the DS2969 (**5**) protected 50% of the mice from death on day 3, only 25% of the mice survived on Day 7. By contrast, all the mice in the groups treated with compound **28** and AZD5099 (**6**) survived. Further experiments proved that compound **28** has a lower median effective dose (ED_{50}) than AZD5099 (**6**) (2.5 mg/kg vs 7.5 mg/kg). It turns out that the hydroxyisopropyl group of pyridazine **28** has unique advantages compared with the other substitutions, which may result in better pharmacokinetic properties *in vivo*.

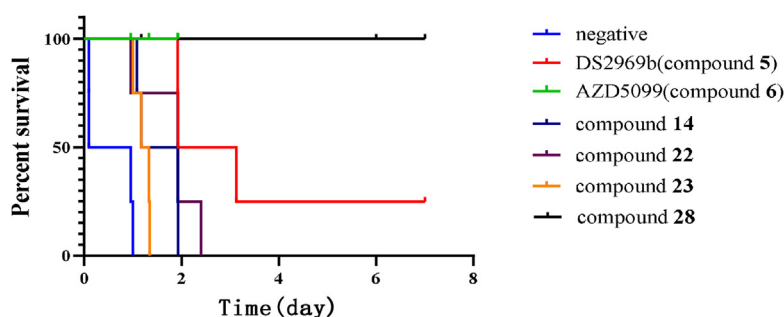


Figure 4 The protective effects *in vivo* of the compounds on a mouse model of sepsis by intragastric administration ($n = 4$ for each group).

2.4. Antibacterial spectrum of compound 28

Then the antibacterial spectrum of compound **28** was assayed, with DS2969 (**5**) and AZD5099 (**6**) as the positive control drugs (Table 5). The quality control strains were purchased from ATCC. The other strains were clinically isolated pathogenic bacteria collected in Sichuan, Beijing, and Shanghai from 2015 to 2020. Compound **28** showed slightly better inhibitory effects than AZD5099 (**6**) against susceptible and resistant Gram-positive bacteria including *S. aureus* (MRSA, MSSA, VISA), *S. epidermidis* (MRSE, MSSE), *E. faecalis* and *E. faecium* strains, with the MIC values less than 0.03 $\mu\text{g}/\text{mL}$, which are potent than DS-2969 (**5**). Moreover, compound **28** also has much better inhibitory activity against Gram-negative bacteria strains, with the MIC value of *P. aeruginosa* (ATCC27853) as 4 $\mu\text{g}/\text{mL}$, *A. baumannii* (ATCC19606) and *K. pneumoniae* (KNP-15-1) as 8 $\mu\text{g}/\text{mL}$. By contrast, AZD5099 (**6**) and DS2969 (**5**) were almost inactive against the assayed strains.

2.5. Evaluation of spontaneous resistance

The frequencies of spontaneous resistance of compound **28** on *S. aureus* (ATCC29213) and methicillin-resistant *S. aureus* (ATCC43300) at 4 \times MIC have been determined, with DS-2969 (**5**) and AZD5099 (**6**) as controls. Compound **28** displayed low spontaneous resistance frequencies of less than 8×10^{-12} and 4.3×10^{-12} on the two strains, similar to the control drugs²⁶.

2.6. Time-killing curves

A time-kill curve of compound **28** against the susceptible *S. aureus* (ATCC29213) was then plotted, with DS-2969 (**5**) and

Table 5 Antibacterial spectrum of compound **28** (MIC $\mu\text{g}/\text{mL}$).

Strains	DS-2969 (5)	AZD5099 (6)	28
<i>S. aureus</i> ATCC43300	0.5	0.03	0.015
<i>S. aureus</i> MRSA15-1 ^a	0.5	0.03	0.015
<i>S. aureus</i> MRSA15-2 ^a	0.5	0.03	0.015
<i>S. aureus</i> MSSA15-1 ^a	0.5	0.03	0.015
<i>S. aureus</i> MSSA15-2 ^a	0.5	0.03	0.015
<i>S. aureus</i> VISA5836	0.5	0.015	0.015
<i>S. aureus</i> VISA5827	0.5	0.015	0.015
<i>S. epidermidis</i> MRSE15-1 ^a	0.25	0.03	0.015
<i>S. epidermidis</i> MRSE15-2 ^a	0.125	0.03	0.015
<i>S. epidermidis</i> MSSE15-3 ^a	0.25	0.03	0.015
<i>E. faecalis</i> ATCC51575	0.5	0.03	0.03
<i>E. faecalis</i> ATCC51299	0.5	0.03	0.015
<i>E. faecium</i> EFM19-1 ^a	0.5	0.03	0.015
<i>P. aeruginosa</i> ATCC27853	>64	>64	4
<i>A. baumannii</i> ATCC19606	>64	>64	8
<i>K. pneumoniae</i> KNP-15-1	>64	>64	8

^aClinically isolated pathogenic bacteria collected in Sichuan, Beijing, and Shanghai from 2015 to 2020.

AZD5099 (**6**) as positive controls (Fig. 5). It showed a time-dependent bactericidal effect at 4, 8, and 16 \times MIC concentrations, similar to DS2969 (**5**) and AZD5099 (**6**).

2.7. Safety evaluation

For pyrrolamide-type GyrB/ParE inhibitors such as AZD5099 (**6**), the mitochondrial toxicity is a worrying deficiency and obstacle. Mitochondrial toxicity was tested *in vitro* using HepG2 cells as reported by Cotman and coworkers³⁰. Although AZD5099 (**6**) showed significant mitochondrial toxicity ($\text{IC}_{50} < 200 \mu\text{mol}/\text{L}$) and resulted in complete damage at 400 $\mu\text{mol}/\text{L}$, compound **28** had much less toxicity at the 50–800 $\mu\text{mol}/\text{L}$, indicating it had much better safety and therapeutic indexes (Fig. 6). Compound **28** also has little inhibitory effect on hERG potassium current ($\text{IC}_{50} > 30 \mu\text{mol}/\text{L}$), indicating a low risk of cardiac QT syndrome. Mini-Ames test proved that this compound did not show any mutagenic effects on *Salmonella typhimurium* TA98 and TA100 strains. It also showed excellent selectivities in human cells such as renal tubular epithelial cell HK2, normal hepatocyte LO2 and embryonic kidney cell HEK293 ($\text{IC}_{50} > 10 \mu\text{mol}/\text{L}$). The mice median lethal doses (LD_{50}) of compound **28** by intragastric administration (ig), intraperitoneal injection (ip) and tail vein injection (iv) were over 800, 300 and 100 mg/kg respectively in acute toxicity tests. The following *in vivo* subacute toxicity studies in mice also showed great drug safety of compound **28** by repeated gavage administration at 150 and 300 mg/kg for one week ($n = 10$ for each group). During this process, no significant damage to the main organs of the mice was found, suggesting it has wide therapeutic indexes.

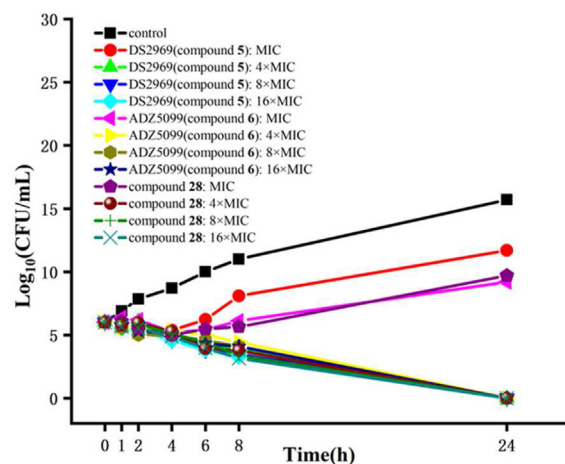


Figure 5 Time-killing curves of compound **28**.

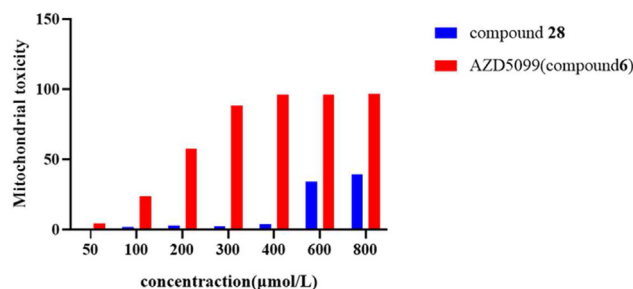


Figure 6 The mitochondrial toxicity assay of the compounds.

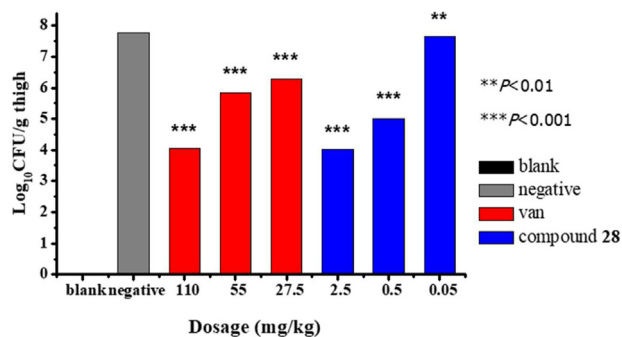


Figure 7 Neutropenic murine thigh infection models ($n = 4$ for each group).

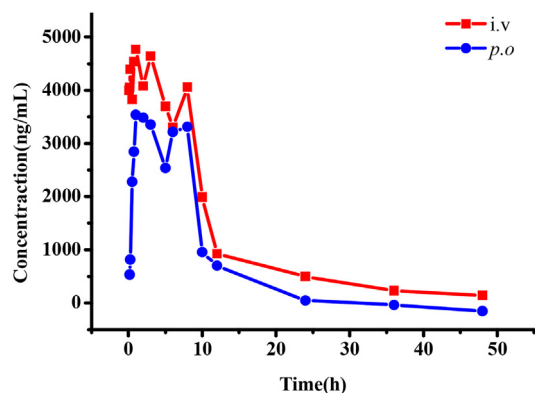


Figure 8 Drug time curve of compound **28** in Beagle dogs.

2.8. Neutropenic murine thigh MRSA infection models

The *in vivo* antibacterial efficacy of compound **28** was evaluated in neutropenic murine thigh MRSA (ATCC43300) infection models with clinically used vancomycin as positive control through tail vein injection administration (iv) (Fig. 7)³². It can be

Table 6 Pharmacokinetic parameters of compound **28** in Beagle dogs.

Parameter	Unit	iv (1 mg/kg)	po (1 mg/kg)
AUC_{0-48}	$\mu\text{g}\cdot\text{h}$	56,432.101	38,552.203
$AUC_{0-\infty}$	$\mu\text{g}\cdot\text{h}$	58,890.621	39,362.651
MRT_{0-48}	h	9.792	9.071
$MRT_{0-\infty}$	h	12.329	9.853
$t_{1/2}$	h	11.285	8.533
T_{max}	h	0.873	1.75
C_{max}	$\mu\text{g/L}$	5510.488	3748.103
CL	$\text{mL}/\text{min}/\text{kg}$	0.33	/
F	—	/	66.84%

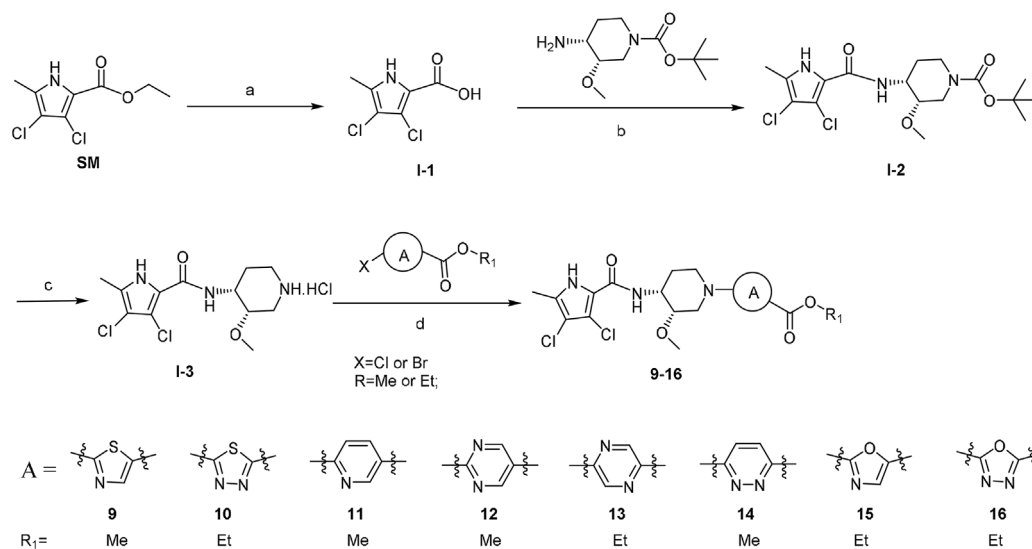
found that compound **28** was efficacious against neutropenic mice thigh infections in a dose-dependent manner from 0.5 to 2.5 mg/kg, resulting in a 3–4- \log_{10} reduction of colony-forming unit (CFU) in the thigh at 2.5 mg/kg. By comparison, vancomycin required a higher effective dose of 110 mg/kg.

2.9. Pharmacokinetics study on beagle dogs

For antibacterial drugs, the pharmacokinetic properties are crucial to antibacterial activities *in vivo*. The pharmacokinetics studies on beagle dogs of compound **28** were performed, which showed fine pharmacokinetics after intravenous injection (iv) and oral administration (po) at 1 mg/kg, with the good absorption ($AUC_{0-48} = 56,432.101$ vs 38,552.203 $\mu\text{g}\cdot\text{h}$) and metabolic stability and low clearance ($t_{1/2} = 11.285$ vs 8.533 h, CL = 0.33 mL/min/kg), as well as high oral bioavailability (66.84%) (Fig. 8, Table 6).

2.10. Chemistry

The starting material ethyl 3,4-dichloro-5-methyl-1H-pyrrole-2-carboxylate was hydrolyzed to carboxylic acid under alkaline conditions to obtain intermediate **I-1** (Scheme 1). Then the chiral 1-*tert*-butoxycarbonyl-3-methoxy-4-aminopiperidine



Scheme 1 Synthesis of compounds **9–16**. Reagents and conditions: (a) i) 3 mol/L NaOH, EtOH, r.t.; ii) HCl (aq), r.t. 85%; (b) HATU, DIPEA, DMSO, r.t. 87%; (c) HCl/1,4-dioxane, 50 °C, 91%; (d) DIPEA, DMF, 60 °C, 70%–90%.

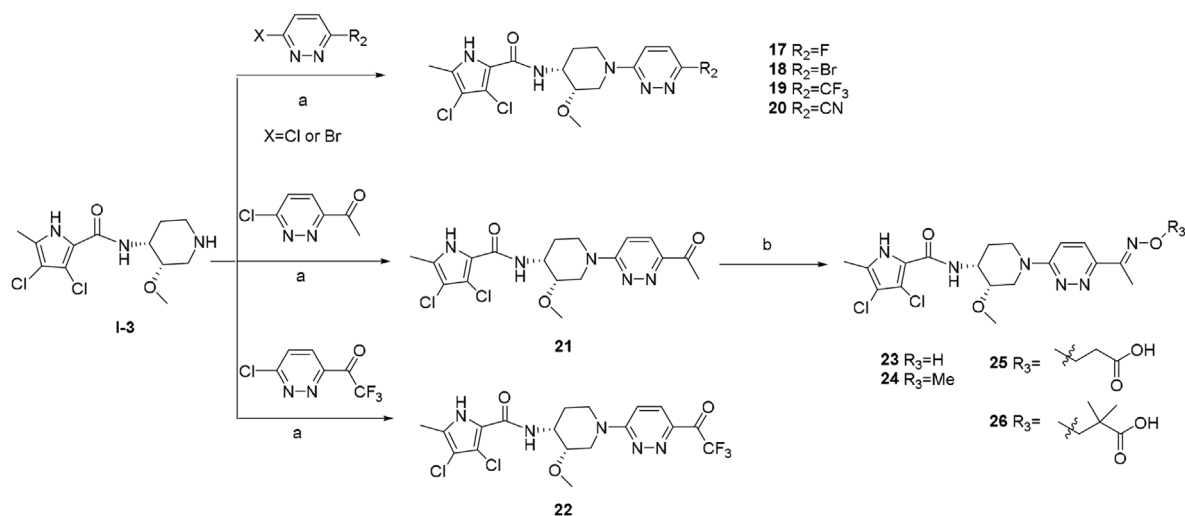
was subjected to an amide condensation reaction with **I-1** under the action of HATU and DIPEA to obtain intermediate **I-2**, followed by the removal of the protective group under the action of HCl/1,4-dioxane to obtain amine **I-3**. It reacted with halogenated heteroaryl formate through nucleophilic substitution reaction to obtain compounds **9–16** in 70%–90% yields.

Under the action of DIPEA, the intermediate **I-3** reacted with a substituted pyridazine ring through a nucleophilic substitution reaction to give fluoro, bromo, trifluoromethyl and cyano compounds **17–20** (Scheme 2). Then the same intermediate **I-3** underwent nucleophilic substitution reaction with 6-chloro-3-acetylpyridazine and 6-chloro-3-trifluoroacetylpyridazine under

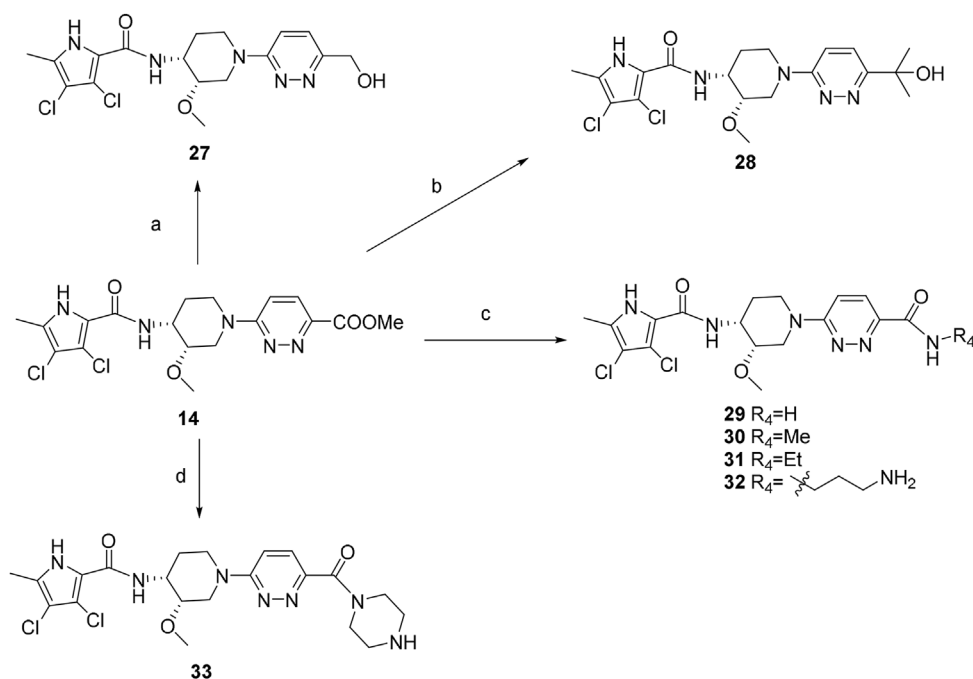
the action of DIPEA to obtain compounds **21** and **22**. Compound **21** reacted with hydroxylamine hydrochloride or its derivatives to obtain compounds **23–26** (Scheme 2).

The methyl ester **14** was reduced by sodium borohydride to give hydroxymethyl compound **27**, and then compound **28** was obtained by Grignard reaction with methyl magnesium bromide (Scheme 3). The amide compounds **29–32** were obtained by aminolysis of ester **14**, while the pyrazinamide compound **33** was obtained through amide condensation with acid.

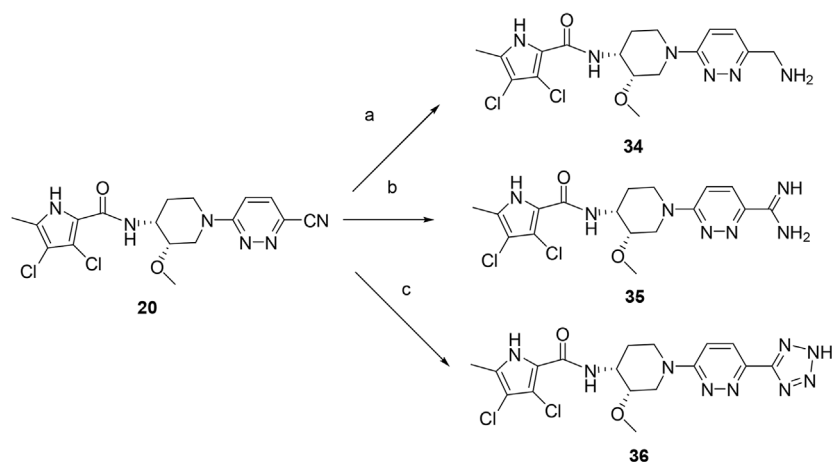
The cyano compound **20** was reduced under the action of palladium–carbon hydrogenation to obtain the primary amine **34** (Scheme 4). After the hydrolysis of compound **20**, the amidino



Scheme 2 Synthesis of compounds **17–26**. Reagents and conditions: (a) DIPEA, DMF, 60 °C, 70%–80%; (b) Hydroxylamine, MeOH, H₂O, 60 °C, 67%–81%.



Scheme 3 Synthesis of compounds **27–33**. Reagents and conditions: (a) NaBH₄, MeOH, 41%, r.t.; (b) CH₃BrMg/THF, –5 °C–r.t., 50%; (c) Amine, MeOH, r.t., 50%–80%; (d) i) 3 mol/L NaOH, MeOH, 70 °C, ii) HCl (aq), r.t. 75%; iii) HATU, DIPEA, r.t. 65%.



Scheme 4 Synthesis of compounds **34**–**36**. Reagents and conditions: (a) H_2 (0.4 MPa), Pd/C, MeOH, 41%; (b) i) NaOCH_3 , MeOH, r.t.; ii) NH_4Cl , MeOH, 65 °C, 56%; (c) NaN_3 , Py, HCl, 110 °C, 45%.

compound **35** was obtained by the following amination reaction. And then compound **20** underwent a cyclization reaction with sodium azide to obtain the tetrazole compound **36**. The chemical structure of the target compounds was confirmed by ^1H NMR, ^{13}C NMR and HR ESI MS, and the purity of the compounds was confirmed by UPLC–MS.

3. Conclusions

ATP-competitive GyrB/ParE are important targets for antibacterial drugs, but since the novobiocin (**1**) has been withdrawn from the market, there is no GyrB/ParE inhibitor yet approved in the clinic. Although a great number of GyrB/ParE inhibitors in different types with excellent antibacterial activities have been reported, there are only three drug candidates in clinical trials currently.

AZD5099, a representative pyrrolamide-type GyrB/ParE inhibitor, was withdrawn from clinical trials because of mitochondrial toxicity and other drug safety issues in 2011. Herein we discovered novel pyrrolamide-type GyrB/ParE inhibitors based on the structural modifications of the AZD5099 (**6**). After systematic replacement of the thiazole and the carboxyl group, the hydroxyisopropyl pyridazine compound **28** with better antibacterial activities and druggability was discovered. Compound **28** had a significant inhibitory effect on Gyrase (GyrB, $\text{IC}_{50} = 49 \text{ nmol/L}$) and a modest inhibitory effect on Topo IV (ParE, $\text{IC}_{50} = 1.513 \text{ }\mu\text{mol/L}$) of *S. aureus*. It also showed significant antibacterial effects against several susceptible or resistant Gram-positive bacteria strains with MIC values below $0.03 \text{ }\mu\text{g/mL}$. The frequencies of spontaneous resistance of this compound on the *S. aureus* bacteria were low. The killing curve showed that this compound had a time-dependent bactericidal effect at concentrations of 4, 8 and $16 \times \text{MIC}$. Compound **28** had better protective effects than DS-2969 (**5**) and AZD5099 (**6**) in mouse models of sepsis induced by MRSA. Moreover, the compound **28** had an obvious bactericidal effect at a dose of 2.5 mg/kg by tail vein injection in mouse thigh infection (MRSA) mode, resulting in 3–4- \log_{10} reductions in CFU in the thigh, and the effective doses were significantly lower than the positive drug vancomycin.

What's more, the compound **28** also has much better safety and a higher therapeutic index than AZD5099 (**6**). It also showed good absorptions, metabolic stabilities as well as oral bioavailability in beagle dogs. At present, compound **28** has been evaluated as a pre-clinical drug candidate for the treatment of drug-resistant Gram-positive bacterial infections.

On the other hand, for Gram-negative bacterial strains, the outer membrane of lipopolysaccharide and the intracellular efflux pumps prevent most antibiotics from entering the cell, so they are less sensitive to antibiotics than Gram-positive bacteria^{33,34}. Therefore, although many compounds with strong inhibitory effects on *E. coli* gyrase and Topo IV have been reported in the literature before, their antibacterial effects on *E. coli* strains are relatively weak^{18–22}. To our delight, compound **28** as well as **14**, **22** and **23** with moderate *E. coli* gyrase inhibitory activities have comparable antibacterial activities against Gram-negative bacteria with the most potent pyrrolamide-type GyrB/ParE inhibitors reported recently^{29,30}. They can be further studied as the lead compounds against drug-resistant Gram-negative bacterial infections.

4. Experimental

4.1. Chemistry

All of the solvents and reagents used were obtained commercially and used without further purification unless noted otherwise. All the reactions were monitored by thin layer chromatography (TLC) on the silica gel plates GF254 and visualized with UV light or iodine vapor. Products were purified by flash chromatography on silica gel (200–300 mesh). ^1H and ^{13}C NMR spectra were recorded on a Varian 400 or 500 NMR spectrometer using chloroform-*d* or DMSO-*d*₆ solutions with tetramethylsilane (TMS) as an internal standard. High-resolution mass spectrometry was conducted by an Agilent Technologies LC/MSD TOF mass spectrometer in positive and negative polarity. All final compounds (compounds **9**–**36**) were determined *via* analysis by Waters UPLC/SQD system using a reversed-phase C18 column with

5%–95% CH₃CN in water (0.1% HCOOH) for 10 min at a flow rate of 0.2 mL/min.

3,4-Dichloro-5-methyl-1H-pyrrole-2-carboxylic acid (I-1). A mixture of 3,4-dichloro-5-methyl-1H-pyrrole-2-carboxylate (3 g, 13.6 mmol), NaOH (1.63 g, 41 mmol) in EtOH (9 mL) and water (15 mL) was heated at 60 °C for about 6 h. After the completion of the reaction determined by TLC, the excess EtOH was removed under reduced pressure. The reaction mixture was acidified with 1 mol/L HCl to pH 2–3 and the residue was extracted with DCM (50 mL × 3). The organic layer was washed with H₂O, dried over Na₂SO₄, filtered, and concentrated under reduced pressure to afford 2.25 g of the **I-1** as a pink solid in 86% yield. ¹H NMR (500 MHz, DMSO-*d*₆) δ 12.78 (s, 1H), 12.17 (s, 1H), 2.18 (s, 3H). ¹³C NMR (126 MHz, DMSO-*d*₆) δ 160.2, 129.3, 116.1, 114.7, 109.1, 10.8.

Tert-butyl((3S,4R)-4-(3,4-dichloro-5-methyl-1H-pyrrole-2-carboxamido)-3-methoxy-piperidine-1-carboxylate (I-2). To a solution of intermediate **I-1** (1 g, 5.2 mmol) in DMSO (6 mL) was added HATU (3 g, 7.7 mmol) and DIPEA (1.3 mL, 7.7 mmol) successively. After stirring at room temperature for 15 min, the chiral **1-tert-butoxycarbonyl-3-methoxy-4-aminopiperidine** (1.4 g, 6.2 mmol) was added and stirring was continued until completion determined by TLC. The reaction mixture was poured into 10 mL water. The resulting precipitate was filtered, washed with 0.1 mol/L HCl and saturated NaHCO₃, filtered, and dried to afford **I-2** (1.8 g, 85%) as a light gray solid. ¹H NMR (500 MHz, DMSO-*d*₆) δ 12.12 (s, 1H), 7.12 (d, *J* = 8.31 Hz, 1H), 4.28–4.16 (m, 1H), 4.13–4.07 (m, 1H), 3.89 (dd, *J* = 48.60, 13.47 Hz, 1H), 3.32 (s, 3H), 2.97–2.72 (m, 2H), 2.18 (s, 3H), 1.63–1.52 (m, 2H), 1.40 (s, 9H). ¹³C NMR (126 MHz, DMSO-*d*₆) δ 157.5, 154.3, 127.8, 118.6, 109.6, 108.1, 78.6, 75.3, 56.4, 48.2, 43.5, 41.5, 28.0, 25.9, 10.6. HR-MS (ESI): *m/z* [M+Na]⁺ calcd for C₁₇H₂₅Cl₂N₃O₄Na 428.1114, found 428.1105.

3,4-Dichloro-N-((3S,4R)-3-methoxypiperidin-4-yl)-5-methyl-1H-pyrrole-2-carboxamide (I-3). The solution of the intermediate **I-2** (1 g, 2.5 mmol) in 1,4-dioxane (12 mL) and 4 mol/L HCl/1,4-dioxane (4 mL) was heated at 50 °C for about 1 h. The precipitate formed was filtered and dried to afford **I-3** (680 mg, 90%) as a white solid. ¹H NMR (400 MHz, DMSO-*d*₆) δ 12.40 (s, 1H), 9.63–9.51 (m, 1H), 8.43 (d, *J* = 9.5 Hz, 1H), 7.39 (d, *J* = 8.2 Hz, 1H), 4.30–4.22 (m, 1H), 3.66–3.63 (m, 1H), 3.54 (d, *J* = 13.1 Hz, 1H), 3.39 (s, 3H), 3.17 (d, *J* = 13.6 Hz, 1H), 3.12–2.95 (m, 2H), 2.19 (s, 3H), 1.86–1.78 (m, 2H). ¹³C NMR (101 MHz, DMSO-*d*₆) δ 158.3, 128.2, 119.0, 111.0, 108.7, 73.7, 57.5, 46.4, 43.1, 42.0, 24.6, 11.1. HRMS (ESI): *m/z* [M+H]⁺ calcd for C₁₂H₁₈Cl₂N₃O₂ 306.0771, found 306.0973.

General procedure A for the synthesis of compounds 9–16. A solution of intermediate **I-3** (1 equiv), halogenated heteroarylformate (1.2 equiv) and DIPEA (2.1 equiv) in DMF was heated at 60 °C for about 2 h. After the completion of the reaction determined by TLC, the reaction mixture was poured into water. The precipitated solid was filtered and dried to afford compounds **9–16**.

Methyl 2-((3S,4R)-4-(3,4-dichloro-5-methyl-1H-pyrrole-2-carboxamido)-3-methoxy piperidin-1-yl)thiazole-5-carboxylate (compound 9). Compound **9** (120 mg, 82%) was prepared as general procedure A from methyl 2-bromothiazole-5-carboxylate as a light yellow solid. UPLC purity 97.75%. ¹H NMR (500 MHz, chloroform-*d*) δ 10.35 (s, 1H), 7.84 (s, 1H), 7.28 (d, *J* = 8.5 Hz, 1H), 4.53 (d, *J* = 13.9 Hz, 1H), 4.31 (tq, *J* = 8.0, 3.8 Hz, 1H), 3.99 (d, *J* = 13.1 Hz, 1H), 3.82 (s, 3H), 3.52 (s, 1H), 3.46 (s, 3H), 3.28–3.20 (m, 1H), 3.17 (d, *J* = 14.4 Hz, 1H), 2.28

(s, 3H), 2.00 (qd, *J* = 12.1, 4.5 Hz, 1H), 1.89 (dt, *J* = 13.4, 4.2 Hz, 1H). ¹³C NMR (101 MHz, chloroform-*d*) δ 174.7, 162.5, 159.0, 148.1, 128.2, 118.2, 116.2, 111.6, 110.4, 75.7, 57.6, 51.9, 48.7, 48.2, 47.6, 26.3, 11.2. HR-MS (ESI): *m/z* [M+H]⁺ calcd for C₁₇H₂₁Cl₂N₄O₄S 447.0655, found 447.0943.

Ethyl 5-((3S,4R)-4-(3,4-dichloro-5-methyl-1H-pyrrole-2-carboxamido)-3-methoxy-piperidin-1-yl)-1,3,4-thiadiazole-2-carboxylate (compound 10). Compound **10** (735 mg, 81%) was prepared as general procedure A from ethyl 5-bromo-1,3,4-thiadiazole-2-carboxylate as a light yellow solid. UPLC purity 96.01%. ¹H NMR (500 MHz, chloroform-*d*) δ 10.71 (s, 1H), 7.30 (d, *J* = 8.4 Hz, 1H), 4.63 (d, *J* = 14.4 Hz, 1H), 4.42 (q, *J* = 7.1 Hz, 2H), 4.31 (tt, *J* = 11.8, 3.9 Hz, 1H), 3.92 (d, *J* = 13.7 Hz, 1H), 3.53 (s, 1H), 3.45 (s, 3H), 3.37 (td, *J* = 13.2, 3.0 Hz, 1H), 3.25 (d, *J* = 14.3 Hz, 1H), 2.26 (s, 3H), 2.02 (tt, *J* = 12.4, 6.2 Hz, 1H), 1.94–1.86 (m, 1H), 1.39 (t, *J* = 7.1 Hz, 3H). ¹³C NMR (101 MHz, chloroform-*d*) δ 174.7, 159.3, 159.1, 149.3, 128.6, 118.1, 111.6, 110.4, 75.64, 62.5, 57.7, 49.8, 49.4, 48.7, 26.3, 14.2, 11.2. HR-MS (ESI): *m/z* [M+H]⁺ calcd for C₁₇H₂₂Cl₂N₅O₄S 460.0619, found 460.0609.

Methyl 6-((3S,4R)-4-(3,4-dichloro-5-methyl-1H-pyrrole-2-carboxamido)-3-methoxy-piperidin-1-yl)nicotinate (compound 11). Compound **11** (170 mg, 79%) was prepared as general procedure A from methyl 6-chloronicotinate (101 mg, 0.59 mmol) as a white solid. ¹H NMR (500 MHz, chloroform-*d*) δ 10.23 (s, 1H), 8.78 (d, *J* = 2.3 Hz, 1H), 8.01 (dd, *J* = 9.0, 2.3 Hz, 1H), 7.29 (d, *J* = 8.4 Hz, 1H), 6.62 (d, *J* = 9.1 Hz, 1H), 5.05 (d, *J* = 14.6 Hz, 1H), 4.34 (qd, *J* = 8.6, 3.2 Hz, 1H), 4.31–4.23 (m, 1H), 3.87 (s, 3H), 3.51 (q, *J* = 1.8 Hz, 1H), 3.42 (s, 3H), 3.12 (ddd, *J* = 14.3, 8.5, 6.8 Hz, 1H), 3.07–2.99 (m, 1H), 2.28 (s, 3H), 1.90 (h, *J* = 4.3, 3.7 Hz, 2H). ¹³C NMR (126 MHz, chloroform-*d*) δ 166.6, 159.0, 151.3, 138.8, 128.0, 118.6, 114.6, 111.5, 110.6, 104.9, 76.4, 57.6, 51.8, 49.3, 44.9, 43.7, 27.1, 11.4. HR-MS (ESI): *m/z* [M+Na]⁺ calcd for C₁₉H₂₂Cl₂N₄O₄Na 463.0910, found 463.0895.

Ethyl 2-((3S,4R)-4-(3,4-dichloro-5-methyl-1H-pyrrole-2-carboxamido)-3-methoxy-piperidin-1-yl)pyrimidine-5-carboxylate (compound 12). Compound **12** (180 mg, 79%) was prepared as general procedure A from ethyl 2-bromopyrimidine-5-carboxylate (139 mg, 0.60 mmol) as a light yellow solid. UPLC purity 96.53%. ¹H NMR (500 MHz, chloroform-*d*) δ 9.77 (s, 1H), 8.83 (s, 2H), 7.27 (s, 1H), 5.32 (m, *J* = 14.4, 2.8 Hz, 1H), 4.98–4.90 (m, 1H), 4.34 (q, *J* = 7.1 Hz, 3H), 3.51 (s, 1H), 3.42 (s, 3H), 3.10–2.98 (m, 2H), 2.28 (s, 3H), 1.84 (m, *J* = 29.2, 16.9, 6.5 Hz, 2H), 1.37 (t, *J* = 7.1 Hz, 3H). ¹³C NMR (101 MHz, DMSO-*d*₆) δ 165.0, 163.0, 159.9, 158.9, 127.9, 118.6, 112.8, 111.5, 110.6, 76.4, 60.7, 57.5, 49.4, 44.3, 42.9, 29.8, 27.3, 14.5, 11.4. HR-MS (ESI): *m/z* [M+Na]⁺ calcd for C₁₉H₂₃Cl₂N₅O₄Na 478.1019, found 478.1029.

Methyl-5-((3S,4R)-4-(3,4-dichloro-5-methyl-1H-pyrrole-2-carboxamido)-3-methoxypiperidin-1-yl)pyrazine-2-carboxylate (compound 13). Compound **13** (173 mg, 78%) was prepared as general procedure A from methyl 5-bromopyrazine-2-carboxylate (130 mg, 0.60 mmol) as a white solid. UPLC purity 96.86%. ¹H NMR (400 MHz, DMSO-*d*₆) δ 12.14 (s, 1H), 8.63 (d, *J* = 1.5 Hz, 1H), 8.45 (d, *J* = 1.5 Hz, 1H), 7.13 (d, *J* = 8.3 Hz, 1H), 4.85 (d, *J* = 14.4 Hz, 1H), 4.50 (d, *J* = 12.2 Hz, 1H), 4.34–4.25 (m, 1H), 3.81 (s, 3H), 3.55 (t, *J* = 2.9 Hz, 1H), 3.32 (s, 3H), 3.26 (d, *J* = 13.7 Hz, 1H), 3.22–3.12 (m, 1H), 2.18 (s, 3H), 1.81–1.74 (m, 1H), 1.71–1.59 (m, 1H). ¹³C NMR (101 MHz, DMSO-*d*₆) δ 165.0, 158.1, 155.8, 144.9, 130.7, 129.7, 128.3, 119.1, 110.1, 108.6, 76.5, 57.5, 52.1, 48.6, 44.8, 42.9, 27.1, 11.1. HR-MS (ESI): *m/z* [M+Na]⁺ calcd for C₁₈H₂₁Cl₂N₅O₄Na 464.0863, found 464.0868.

Methyl-6-((3S,4R)-4-(3,4-dichloro-5-methyl-1H-pyrrole-2-carboxamido)-3-methoxypiperidin-1-yl)pyridazine-3-carboxylate (compound 14). Compound **14** (850 mg, 72%) was prepared as general procedure A from methyl 6-bromopyridazine-3-carboxylate (700 mg, 3.20 mmol) as a white solid. UPLC purity 97.14%. ¹H NMR (500 MHz, chloroform-*d*) δ 9.54 (s, 1H), 7.88 (d, $J = 9.7$ Hz, 1H), 7.25 (s, 1H), 6.89 (d, $J = 9.5$ Hz, 1H), 5.38 (d, $J = 13.9$ Hz, 1H), 4.37 (s, 1H), 4.24 (d, $J = 13.4$ Hz, 1H), 4.00 (s, 3H), 3.56 (s, 1H), 3.43 (s, 3H), 3.25–3.17 (m, 1H), 3.10 (d, $J = 14.9$ Hz, 1H), 2.28 (s, 3H), 1.99–1.86 (m, 2H). ¹³C NMR (101 MHz, chloroform-*d*) δ 165.1, 160.1, 158.8, 142.6, 128.8, 128.0, 118.4, 111.5, 110.5, 109.9, 76.1, 57.6, 52.6, 49.1, 44.6, 43.7, 26.9, 11.3. HR-MS (ESI): m/z [M+Na]⁺ calcd for C₁₈H₂₁Cl₂N₅O₄Na 464.0863, found 464.0873.

Ethyl-2-((3S,4R)-4-(3,4-dichloro-5-methyl-1H-pyrrole-2-carboxamido)-3-methoxy-piperidin-1-yl)oxazole-5-carboxylate (compound 15). Compound **15** (147 mg, 90%) was prepared as general procedure A from ethyl 2-bromooxazole-5-carboxylate (80 mg, 0.36 mmol) as a white solid. UPLC purity 98.08%. ¹H NMR (500 MHz, chloroform-*d*) δ 10.30 (s, 1H), 7.52 (s, 1H), 7.25 (d, $J = 4.6$ Hz, 1H), 4.55 (d, $J = 14.4$ Hz, 1H), 4.32–4.28 (m, 2H), 4.26 (d, $J = 11.4$ Hz, 2H), 3.48 (d, $J = 1.4$ Hz, 1H), 3.44 (s, 3H), 3.18–3.07 (m, 2H), 2.26 (s, 3H), 1.95 (qd, $J = 12.4$, 4.5 Hz, 1H), 1.85 (d, $J = 10.4$ Hz, 1H), 1.33 (t, $J = 7.1$ Hz, 3H). ¹³C NMR (126 MHz, chloroform-*d*) δ 163.1, 159.0, 158.1, 136.9, 136.6, 128.2, 118.4, 111.60, 110.6, 75.61, 60.7, 57.5, 48.7, 46.0, 44.6, 26.6, 14.5, 11.4. HR-MS (ESI): m/z [M+Na]⁺ calcd for C₁₈H₂₂Cl₂N₄O₅Na 467.0859, found 467.0856.

Ethyl-5-((3S,4R)-4-(3,4-dichloro-5-methyl-1H-pyrrole-2-carboxamido)-3-methoxy piperidin-1-yl)-1,3,4-oxadiazole-2-carboxylate (compound 16). Compound **16** (219 mg, 87%) was prepared as general procedure A from ethyl 5-bromo-1,3,4-oxadiazole-2-carboxylate (150 mg, 0.68 mmol) as a light yellow solid. UPLC purity 95.91%. ¹H NMR (500 MHz, chloroform-*d*) δ 9.71 (s, 1H), 7.22 (d, $J = 8.8$ Hz, 1H), 4.53–4.41 (m, 3H), 4.33–4.26 (m, 1H), 4.22 (d, $J = 13.5$ Hz, 1H), 3.51 (s, 1H), 3.45 (s, 3H), 3.27–3.17 (m, 2H), 2.27 (s, 3H), 1.97 (m, $J = 12.4$, 6.5 Hz, 1H), 1.91–1.85 (m, 1H), 1.42 (t, $J = 7.1$ Hz, 3H). ¹³C NMR (101 MHz, chloroform-*d*) δ 165.2, 158.7, 154.5, 151.3, 128.0, 118.3, 111.5, 110.56, 75.4, 62.8, 57.5, 48.4, 46.6, 45.2, 26.3, 14.2, 11.3. HR-MS (ESI): m/z [M–H][–] calcd for C₁₇H₂₀Cl₂N₅O₅ 444.0847, found 444.0836.

3,4-Dichloro-N-((3S,4R)-1-(6-fluoropyridazin-3-yl)-3-methoxy piperidin-4-yl)-5-methyl-1H-pyrrole-2-carboxamide (compound 17). Compound **17** (40 mg, 70%) was prepared as general procedure A for 3,6-difluoropyridazine (20 mg, 0.17 mmol) as a white solid. UPLC purity 97.24%. ¹H NMR (500 MHz, chloroform-*d*) δ 9.93 (s, 1H), 7.29 (s, 1H), 7.13–7.08 (m, 1H), 7.00 (d, $J = 9.7$ Hz, 1H), 4.85 (d, $J = 14.5$ Hz, 1H), 4.33 (d, $J = 5.4$ Hz, 1H), 4.11 (d, $J = 14.0$ Hz, 1H), 3.54 (s, 1H), 3.42 (d, $J = 1.5$ Hz, 3H), 3.10 (dd, $J = 35.3$, 14.3 Hz, 2H), 2.31–2.25 (m, 3H), 2.00–1.89 (m, 2H). ¹³C NMR (101 MHz, chloroform-*d*) δ 161.2 (d, $J_{C-F} = 235.3$ Hz), 159.7, 158.8, 127.9, 118.4, 117.3, 116.9, 111.4, 110.4, 76.2, 57.5, 48.9, 45.8, 44.6, 26.7, 11.3. HR-MS (ESI): m/z [M+Na]⁺ calcd for C₁₆H₁₈Cl₂FN₅O₂Na 424.0714, found 424.0726.

N-((3S,4R)-1-(6-Bromopyridazin-3-yl)-3-methoxypiperidin-4-yl)-3,4-dichloro-5-methyl-1H-pyrrole-2-carboxamide (compound 18). Compound **18** (233 mg, 74%) was prepared as general procedure A from 3,6-dibromopyridazine (195 mg, 0.82 mmol) as a white solid. UPLC purity 95.90%. ¹H NMR (500 MHz, chloroform-*d*) δ 10.06 (s, 1H), 7.32–7.26 (m, 2H), 6.82 (d, $J = 9.6$ Hz, 1H), 4.97 (d, $J = 14.4$ Hz, 1H), 4.41–4.30 (m, 1H), 4.12 (d,

$J = 13.9$ Hz, 1H), 3.53 (s, 1H), 3.45–3.40 (m, 3H), 3.12 (ddd, $J = 13.5$, 9.8, 4.9 Hz, 1H), 3.05 (d, $J = 14.6$ Hz, 1H), 2.28 (s, 3H), 1.95–1.88 (m, 2H). ¹³C NMR (101 MHz, DMSO-*d*₆) δ 160.0, 158.1, 136.4, 132.1, 128.4, 119.2, 116.7, 110.0, 108.6, 76.5, 57.3, 48.6, 45.4, 43.2, 26.7, 11.1. HR-MS (ESI): m/z [M+Na]⁺ calcd for C₁₆H₁₈BrCl₂N₅O₂Na 483.9913, found 483.9925.

3,4-Dichloro-N-((3S,4R)-3-methoxy-1-(6-(trifluoromethyl)pyridazin-3-yl)piperidin-4-yl)-5-methyl-1H-pyrrole-2-carboxamide (compound 19). Compound **19** (70 mg, 77%) was prepared as general procedure A from 3-chloro-6-(trifluoromethyl)pyridazine (44 mg, 0.24 mmol) as a white solid. UPLC purity 99.90%. ¹H NMR (500 MHz, chloroform-*d*) δ 9.99–9.89 (m, 1H), 7.47 (dd, $J = 9.6$, 4.2 Hz, 1H), 7.30 (d, $J = 4.9$ Hz, 1H), 6.95 (dd, $J = 9.7$, 4.4 Hz, 1H), 5.25 (d, $J = 14.7$ Hz, 1H), 4.44–4.33 (m, 1H), 4.31–4.21 (m, 1H), 3.57 (s, 1H), 3.44 (d, $J = 4.1$ Hz, 3H), 3.19 (t, $J = 12.8$ Hz, 1H), 3.11 (dd, $J = 15.0$, 4.4 Hz, 1H), 2.29 (d, $J = 4.2$ Hz, 3H), 2.00–1.87 (m, 2H). ¹³C NMR (101 MHz, chloroform-*d*) δ 160.5, 158.8, 142.5 (q, $J_{C-CF_3} = 34.0$ Hz), 128.0, 124.7, 122.1 (d, $J_{C-F} = 271.0$ Hz), 118.4, 111.5, 110.8, 110.5, 76.2, 57.7, 49.0, 44.8, 43.7, 26.8, 11.3. HR-MS (ESI): m/z [M+Na]⁺ calcd for C₁₇H₁₈Cl₂F₃N₅O₂Na 474.0682, found 474.0695.

3,4-Dichloro-N-((3S,4R)-1-(6-cyanopyridazin-3-yl)-3-methoxy piperidin-4-yl)-5-methyl-1H-pyrrole-2-carboxamide (compound 20). Compound **20** (97 mg, 72%) was prepared as general procedure A from 6-chloropyridazine-3-carbonitrile (56 mg, 0.40 mmol) as a white solid. UPLC purity 97.96%. ¹H NMR (500 MHz, chloroform-*d*) δ 9.70 (s, 1H), 7.44 (d, $J = 9.6$ Hz, 1H), 7.24 (s, 1H), 6.87 (d, $J = 9.6$ Hz, 1H), 5.28 (d, $J = 11.3$ Hz, 1H), 4.43–4.34 (m, 1H), 4.32–4.21 (m, 1H), 3.57 (s, 1H), 3.42 (s, 3H), 3.21 (t, $J = 12.0$ Hz, 1H), 3.11 (d, $J = 14.5$ Hz, 1H), 2.28 (s, 3H), 2.00–1.83 (m, 2H). ¹³C NMR (101 MHz, chloroform-*d*) δ 159.0, 158.7, 130.64, 129.0, 127.9, 118.3, 116.8, 111.5, 110.6, 109.4, 76.2, 57.7, 48.9, 44.8, 43.7, 26.8, 11.3. HR-MS (ESI): m/z [M–H][–] calcd for C₁₇H₁₇Cl₂N₆O₂ 407.0796, found 407.0784.

N-((3S,4R)-1-(6-Acetylpyridazin-3-yl)-3-methoxypiperidin-4-yl)-3,4-dichloro-5-methyl-1H-pyrrole-2-carboxamide (compound 21). A mixture of 1-(6-chloropyridazin-3-yl)ethan-1-one (40 mg, 0.26 mmol), **I-3** (80 mg, 0.26 mmol) and DIPEA (106 μ L, 0.64 mmol) was heated to 60 °C for about 2 h. After the completion of the reaction determined by TLC, the reaction mixture was poured into water. The precipitated solid was filtered to afford compound **21** (86 mg, 78%) as a white solid. UPLC purity 99.12%. ¹H NMR (500 MHz, chloroform-*d*) δ 10.05 (s, 1H), 7.89 (d, $J = 9.7$ Hz, 1H), 7.28 (d, $J = 8.7$ Hz, 1H), 6.94 (d, $J = 9.7$ Hz, 1H), 5.21 (d, $J = 15.1$ Hz, 1H), 4.44–4.33 (m, 2H), 3.58 (d, $J = 3.4$ Hz, 1H), 3.44 (s, 3H), 3.24–3.10 (m, 2H), 2.77 (s, 3H), 2.28 (s, 3H), 1.99–1.91 (m, 2H). ¹³C NMR (101 MHz, DMSO-*d*₆) δ 197.3, 160.7, 158.1, 148.7, 128.4, 125.9, 119.1, 112.0, 110.1, 108.6, 76.5, 57.5, 48.7, 45.1, 43.1, 27.0, 25.6, 11.1. HR-MS (ESI): m/z [M–H][–] calcd for C₁₇H₂₁Cl₂N₅O₃ 424.0949, found 424.0931.

3,4-Dichloro-N-((3S,4R)-3-methoxy-1-(6-(2,2,2-trifluoroacetyl)pyridazin-3-yl) piperidin-4-yl)-5-methyl-1H-pyrrole-2-carboxamide (compound 22). A mixture of 1-(6-chloropyridazin-3-yl)-2,2,2-trifluoroethan-1-one (100 mg, 0.39 mmol), **I-3** (119 mg, 0.39 mmol) and DIPEA (171 μ L, 0.98 mmol) was heated to 60 °C for about 2 h. After the completion of the reaction determined by TLC, the mixture was extracted with EA (10 mL \times 3). The organic phase was dried over Na₂SO₄ and concentrated under reduced pressure. The residue was

purified by chromatography on silica gel to afford compound **22** (130 mg, 70%) as a yellow solid. UPLC purity 97.00%. ¹H NMR (400 MHz, chloroform-*d*) δ 10.01 (s, 1H), 7.92 (d, *J* = 9.8 Hz, 1H), 7.25 (s, 1H), 6.95 (d, *J* = 9.8 Hz, 1H), 4.44–4.35 (m, 1H), 3.62–3.58 (m, 1H), 3.44 (s, 3H), 3.28–3.16 (m, 2H), 2.95 (s, 1H), 2.88 (d, *J* = 0.6 Hz, 1H), 2.28 (s, 3H), 2.02–1.89 (m, 2H). ¹³C NMR (101 MHz, chloroform-*d*) δ 178.7 (q, *J*_{C-CF₃} = 35.0 Hz), 159.6, 158.8, 144.3, 128.60, 128.1, 118.3, 116.9 (q, *J*_{C-F₃} = 288.0 Hz), 111.6, 110.6, 110.0, 76.3, 57.9, 48.9, 45.1, 43.9, 27.0, 11.3. HR-MS (ESI): *m/z* [M–H][–] calcd for C₁₈H₁₇Cl₂F₃N₅O₃ 478.0666, found 478.0658.

3,4-Dichloro-N-((3S,4R)-1-(6-((E)-1-(hydroxyimino)ethyl)pyridazin-3-yl)-3-methoxypiperidin-4-yl)-5-methyl-1H-pyrrole-2-carboxamide (compound 23). To a solution of compound **21** (60 mg, 0.14 mmol) in MeOH (2 mL) was added hydroxylamine hydrochloride solution (1.5 g dissolved in 2 mL water and 1 mL MeOH). The mixture was stirred at 60 °C. After the completion of the reaction determined by TLC, the reaction mixture was poured into water (8 mL), and extracted with EA (10 ml × 3). The combined organic layer was dried over anhydrous Na₂SO₄ and concentrated under reduced pressure. The residue was purified by chromatography on silica gel to afford compound **23** (50 mg, 81%) as a white solid. UPLC purity 99.90%. ¹H NMR (500 MHz, DMSO-*d*₆) δ 12.15 (s, 1H), 11.38 (s, 1H), 7.70 (d, *J* = 9.7 Hz, 1H), 7.33 (d, *J* = 9.9 Hz, 1H), 7.13 (d, *J* = 8.2 Hz, 1H), 4.69 (d, *J* = 14.7 Hz, 1H), 4.40 (d, *J* = 12.6 Hz, 1H), 4.26 (d, *J* = 2.8 Hz, 1H), 3.49 (s, 1H), 3.21 (d, *J* = 14.3 Hz, 1H), 3.16–3.07 (m, 1H), 2.48 (s, 3H), 2.22 (s, 3H), 2.16 (s, 3H), 1.76–1.65 (m, 2H). ¹³C NMR (101 MHz, DMSO-*d*₆) δ 159.9, 158.1, 153.1, 148.5, 128.3, 124.7, 119.2, 113.3, 110.1, 108.6, 76.5, 57.3, 48.7, 45.1, 43.0, 26.9, 11.1, 10.3. HR-MS (ESI): *m/z* [M–H][–] calcd for C₁₈H₂₁Cl₂N₆O₃ 439.1058, found 439.1042.

3,4-Dichloro-N-((3S,4R)-3-methoxy-1-(6-((E)-1-(methoxyimino)ethyl)pyridazin-3-yl)piperidin-4-yl)-5-methyl-1H-pyrrole-2-carboxamide (compound 24). Compound **24** (32 mg, 78%) was prepared from compound **21** (40 mg, 0.09 mmol) and methoxyammonium chloride (0.75 g dissolved in 2 mL water and 1 mL MeOH) in the same manner as described for compound **23** as a white solid. ¹H NMR (500 MHz, chloroform-*d*) δ 10.40 (s, 1H), 7.90–7.82 (m, 1H), 7.31 (d, *J* = 8.4 Hz, 1H), 6.91 (d, *J* = 9.7 Hz, 1H), 5.05–4.96 (m, 1H), 4.35 (m, 1H), 4.28 (d, *J* = 12.8 Hz, 1H), 4.00 (d, *J* = 1.6 Hz, 3H), 3.55 (d, *J* = 3.4 Hz, 1H), 3.42 (s, 3H), 3.18–3.07 (m, 2H), 2.38 (d, *J* = 1.6 Hz, 3H), 2.28 (s, 3H), 1.94 (m, 2H). ¹³C NMR (101 MHz, DMSO-*d*₆) δ 159.5, 159.0, 154.1, 148.5, 128.1, 125.5, 118.5, 112.3, 111.5, 110.5, 76.3, 62.4, 57.7, 49.2, 45.2, 43.8, 27.0, 11.4, 10.5. HR-MS (ESI): *m/z* [M+H]⁺ calcd for C₁₉H₂₅Cl₂N₆O₃ 455.1360, found 455.1378.

2-(((E)-1-(6-((3S,4R)-4-(3,4-Dichloro-5-methyl-1H-pyrrole-2-carboxamido)-3-methoxypiperidin-1-yl)pyridazine-3-yl)ethylidene)amino)oxy)acetic acid (compound 25). Compound **25** (33 mg, 70%) was prepared from compound **21** (40 mg, 0.09 mmol) and 2-(aminoxy)acetic acid (200 mg dissolved in 1 mL water and 1 mL MeOH) in the same manner as described for compound **23** as a white solid. ¹H NMR (500 MHz, DMSO-*d*₆) δ 12.37 (s, 1H), 7.71 (d, *J* = 9.7 Hz, 1H), 7.38 (d, *J* = 9.7 Hz, 1H), 7.28 (d, *J* = 8.3 Hz, 1H), 4.74 (d, *J* = 14.5 Hz, 1H), 4.57 (s, 2H), 4.47 (d, *J* = 12.9 Hz, 1H), 4.33 (d, *J* = 7.4 Hz, 1H), 3.55 (s, 2H), 3.31 (s, 1H), 3.28 (s, 1H), 3.21 (dd, *J* = 16.8, 6.8 Hz, 2H), 2.35 (s, 3H), 2.23 (s, 3H), 1.76 (dd, *J* = 14.1, 9.2 Hz, 2H). ¹³C NMR (101 MHz, DMSO-*d*₆) δ 171.6, 160.1, 158.1, 154.8, 147.2, 128.3, 125.0, 119.2, 113.1, 110.2, 108.6, 76.5, 71.4, 57.3, 48.7,

45.1, 43.0, 39.4, 26.8, 11.1. HR-MS (ESI): *m/z* [M+H]⁺ calcd for C₂₀H₂₅Cl₂N₆O₅ 499.1258, found 499.1273.

2-(((E)-1-(6-((3S,4R)-4-(3,4-Dichloro-5-methyl-1H-pyrrole-2-carboxamido)-3-methoxy piperidin-1-yl)pyridazin-3-yl)ethylidene)amino)oxy)-2-methylpropanoic acid (compound 26). Compound **26** (42 mg, 67%) was prepared from compound **21** (50 mg, 0.12 mmol) and 1-carboxy-1-methylethoxyammonium chloride (100 mg dissolved in 0.5 mL water and 1 mL MeOH) in the same manner as described for compound **23** as a white solid. UPLC purity 98.37%. ¹H NMR (400 MHz, DMSO-*d*₆) δ 12.56 (s, 1H), 12.14 (s, 1H), 7.64 (d, *J* = 9.7 Hz, 1H), 7.38 (d, *J* = 9.8 Hz, 1H), 7.14 (d, *J* = 8.3 Hz, 1H), 4.76–4.66 (m, 1H), 4.44 (d, *J* = 12.7 Hz, 1H), 4.34–4.25 (m, 1H), 3.52 (s, 1H), 3.30 (s, 3H), 2.89 (s, 1H), 2.73 (s, 1H), 2.29 (s, 3H), 2.18 (s, 3H), 1.79–1.67 (m, 2H), 1.50 (s, 6H). ¹³C NMR (101 MHz, DMSO-*d*₆) δ 175.2, 162.8, 159.9, 158.1, 153.8, 147.6, 128.4, 125.1, 119.2, 110.0, 108.5, 81.8, 76.5, 57.4, 48.7, 45.2, 43.1, 36.3, 31.2, 26.9, 24.4, 10.9. HR-MS (ESI): *m/z* [M+H]⁺ calcd for C₂₂H₂₉Cl₂N₆O₅ 527.1571, found 527.1571.

3,4-Dichloro-N-((3S,4R)-1-(6-(hydroxymethyl)pyridazin-3-yl)-3-methoxy piperidin-4-yl)-5-methyl-1H-pyrrole-2-carboxamide (compound 27). To a solution of compound **14** (60 mg, 0.14 mmol) in MeOH (2 mL) was added sodium borohydride (15 mg, 0.41 mmol) in portions at 0 °C and stirred at room temperature for 4 h. After the completion of the reaction determined by TLC, 8 mL water was added to the reaction solution and the mixture was extracted with DCM (10 mL × 3). The organic layer was washed with brine, dried over Na₂SO₄, and concentrated under reduced pressure. The crude residue was purified by chromatography on silica gel to obtain compound **27** (24 mg, 41%) as a white solid. UPLC purity 95.94%. ¹H NMR (500 MHz, chloroform-*d*) δ 10.02 (s, 1H), 7.28 (d, *J* = 8.2 Hz, 1H), 7.24 (d, *J* = 9.4 Hz, 1H), 6.99 (d, *J* = 9.5 Hz, 1H), 4.95 (dt, *J* = 14.5, 3.2 Hz, 1H), 4.80 (s, 2H), 4.37–4.30 (m, 1H), 4.23–4.16 (m, 1H), 3.54 (s, 1H), 3.42 (s, 3H), 3.11 (dd, *J* = 26.4, 11.5 Hz, 2H), 2.28 (s, 3H), 1.95–1.89 (m, 2H). ¹³C NMR (101 MHz, chloroform-*d*) δ 156.0, 158.9, 151.8, 127.9, 126.6, 118.6, 113.6, 111.5, 76.3, 63.5, 57.6, 49.1, 45.3, 44.0, 29.9, 26.9, 11.4. HR-MS (ESI): *m/z* [M–H][–] calcd for C₁₇H₂₀Cl₂N₅O₃ 412.0949, found 412.0941.

3,4-Dichloro-N-((3S,4R)-1-(6-(2-hydroxypropan-2-yl)pyridazin-3-yl)-3-methoxypiperidin-4-yl)-5-methyl-1H-pyrrole-2-carboxamide (compound 28). To a suspension of compound **14** (400 mg, 0.91 mmol) in anhydrous THF (5 mL) was added CH₃BrMg (1.70 mL, 4.60 mmol, 3 mol/L in diethyl ether solution) dropwise under argon at –5 °C. The reaction mixture was stirred at room temperature for 1.5 h, then quenched with saturated NH₄Cl and diluted with water, extracted 3 times with EA. The combined organic layer was washed with brine, dried over anhydrous Na₂SO₄, filtered, and evaporated under reduced pressure. The residue was purified by silica gel column chromatography (CH₂Cl₂/MeOH = 20/1) to afford compound **28** (184 mg, 46%) as a white solid. UPLC purity 98.87%. ¹H NMR (500 MHz, chloroform-*d*) δ 9.58 (s, 1H), 7.36 (d, *J* = 9.6 Hz, 1H), 7.25 (s, 1H), 6.99 (d, *J* = 9.6 Hz, 1H), 4.91 (dd, *J* = 15.0, 2.8 Hz, 1H), 4.35 (dq, *J* = 6.4, 3.1 Hz, 2H), 4.20 (d, *J* = 13.6 Hz, 1H), 3.60–3.54 (m, 1H), 3.44 (s, 3H), 3.18–3.08 (m, 2H), 2.28 (s, 3H), 2.00–1.90 (m, 2H), 1.57 (s, 6H). ¹³C NMR (101 MHz, chloroform-*d*) δ 159.3, 159.0, 158.2, 128.2, 124.6, 118.3, 113.8, 111.4, 110.3, 76.1, 71.6, 57.5, 49.0, 45.2, 43.8, 30.4, 29.7, 26.8, 11.2. HR-MS (ESI): *m/z* [M+H]⁺ calcd for C₁₉H₂₆Cl₂N₅O₃ 442.1407, found 442.1425.

6-((3*S*,4*R*)-4-(3,4-Dichloro-5-methyl-1*H*-pyrrole-2-carboxamido)-3-methoxy piperidin-1-yl)pyridazine-3-carboxamide (compound **29**). To the solution of compound **14** (60 mg, 0.14 mmol) in MeOH (2 mL) was added the ammonia (1 mL, 7 mol/L in MeOH) and the mixture was stirred at room temperature. After the completion of the reaction determined by TLC, the mixture was concentrated under reduced pressure, and the residue was purified by chromatography on silica gel to afford compound **29** (39 mg, 66%) as a white solid. UPLC purity 99.32%. ¹H NMR (500 MHz, DMSO-*d*₆) δ 12.21 (s, 1H), 8.12 (s, 1H), 7.75 (d, *J* = 9.5 Hz, 1H), 7.48 (s, 1H), 7.37 (d, *J* = 9.6 Hz, 1H), 7.16 (d, *J* = 8.2 Hz, 1H), 4.79 (d, *J* = 13.6 Hz, 1H), 4.42 (d, *J* = 12.3 Hz, 1H), 4.25 (s, 1H), 3.48 (s, 1H), 3.21 (s, 1H), 3.14 (t, *J* = 10.8 Hz, 1H), 2.13 (s, 3H), 1.95 (d, *J* = 8.4 Hz, 1H), 1.74–1.61 (m, 2H), 1.18 (s, 2H). ¹³C NMR (101 MHz, DMSO-*d*₆) δ 165.8, 160.9, 158.1, 144.8, 128.3, 126.7, 119.1, 112.6, 110.3, 108.6, 76.4, 57.3, 48.7, 45.0, 43.0, 26.9, 11.1. HR-MS (ESI): *m/z* [M+Na]⁺ calcd for C₁₇H₂₀Cl₂N₆O₃Na 449.0866, found 449.0863.

6-((3*S*,4*R*)-4-(3,4-Dichloro-5-methyl-1*H*-pyrrole-2-carboxamido)-3-methoxy piperidin-1-yl)-*N*-methylpyridazine-3-carboxamide (compound **30**). Compound **30** (43 mg, 70%) was prepared from compound **14** (60 mg, 0.14 mmol) and methylamine (1 mL, 30% in alcohol) in the same manner as described for compound **29** as a white solid. ¹H NMR (500 MHz, chloroform-*d*) δ 10.08 (s, 1H), 8.00 (d, *J* = 9.5 Hz, 1H), 7.87 (d, *J* = 4.7 Hz, 1H), 7.28 (d, *J* = 8.7 Hz, 1H), 6.99 (d, *J* = 9.6 Hz, 1H), 5.09 (d, *J* = 15.2 Hz, 1H), 4.41–4.29 (m, 2H), 3.60–3.53 (m, 1H), 3.42 (s, 3H), 3.21–3.09 (m, 2H), 3.03 (d, *J* = 5.1 Hz, 3H), 2.28 (s, 3H), 1.74 (s, 2H). ¹³C NMR (101 MHz, chloroform-*d*) δ 164.0, 160.5, 158.9, 144.5, 128.0, 126.8, 118.4, 111.7, 111.44, 110.5, 76.2, 57.6, 49.0, 45.1, 43.6, 26.8, 26.1, 11.3. HR-MS (ESI): *m/z* [M-H]⁻ calcd for C₁₈H₂₁Cl₂N₆O₃ 439.1058, found 439.1053.

6-((3*S*,4*R*)-4-(3,4-Dichloro-5-methyl-1*H*-pyrrole-2-carboxamido)-3-methoxypiperidin-1-yl)-*N*-ethylpyridazine-3-carboxamide (compound **31**). To a solution of compound **14** (100 mg, 0.22 mmol) in MeOH (2 mL) and DCM (1 mL) was added 3 mol/L NaOH (1 mL, 3 mmol) and heated to 70 °C for 3 h. The solvent was removed under reduced pressure, the residue was acidified with 1 mol/L HCl to pH 3, and the precipitate solids were collected to give the carboxylic acid (70 mg, 75%) as a pink solid.

To a solution of the above intermediate (50 mg, 0.12 mmol) in DMSO (2 mL) was added HATU (68 mg, 0.18 mmol) and DIPEA (30 μL, 0.18 mmol) successively. After stirring at temperature for 15 min, ethylamine (70 μL, 0.14 mmol, 2 mol/L in THF) was added and stirring was continued until completion determined by TLC. The reaction mixture was poured into 2 mL water. The resulting precipitate was filtered, washed with 0.1 mol/L HCl and saturated NaHCO₃ to afford compound **31** (34 mg, 63%) as a light yellow solid. ¹H NMR (400 MHz, DMSO-*d*₆) δ 12.14 (s, 1H), 8.82 (t, *J* = 6.0 Hz, 1H), 7.79 (d, *J* = 9.5 Hz, 1H), 7.40 (d, *J* = 9.5 Hz, 1H), 7.14 (d, *J* = 8.4 Hz, 1H), 4.86 (d, *J* = 14.3 Hz, 1H), 4.45 (d, *J* = 12.7 Hz, 1H), 4.34–4.23 (m, 1H), 3.54 (s, 1H), 3.30 (s, 3H), 3.28–3.21 (m, 2H), 3.17 (d, *J* = 10.4 Hz, 1H), 2.69 (s, 1H), 2.18 (s, 3H), 1.81–1.64 (m, 2H), 1.12 (t, *J* = 7.2 Hz, 3H). ¹³C NMR (101 MHz, DMSO-*d*₆) δ 163.3, 160.9, 158.1, 144.8, 128.37, 126.5, 119.2, 112.6, 110.1, 108.6, 76.5, 57.3, 48.7, 45.0, 43.1, 34.0, 26.9, 15.4, 11.1. HR-MS (ESI): *m/z* [M+H]⁺ calcd for C₁₉H₂₅Cl₂N₆O₃ 455.1360, found 455.1382.

N-(2-Aminoethyl)-6-((3*S*,4*R*)-4-(3,4-dichloro-5-methyl-1*H*-pyrrole-2-carboxamido)-3-methoxypiperidin-1-yl)pyridazine-3-carboxamide (compound **32**). To a solution of compound **14** (60 mg,

0.14 mmol) in EtOH (2 mL) was added (2-aminoethyl) *tert*-butyl carbamate (110 mg, 0.68 mmol) and the mixture was stirred at room temperature. After the completion of the reaction determined by TLC, the reaction solution was concentrated under reduced pressure, and the residue was purified by chromatography on silica gel to afford 45 mg of the white solid in a 56% yield. The above intermediate (30 mg, 0.05 mmol) was heated at 50 °C for 1 h in a solution of 1,4-dioxane (1 mL) and 4 mol/L HCl/1,4-dioxane (0.5 mL). The precipitate was filtered and dried to afford compound **32** (22 mg, 90%) as a white solid. UPLC purity 98.43%. ¹H NMR (500 MHz, DMSO-*d*₆) δ 12.31 (s, 1H), 9.07 (s, 1H), 8.09 (s, 3H), 7.88 (d, *J* = 9.3 Hz, 1H), 7.56 (d, *J* = 9.7 Hz, 1H), 7.24 (d, *J* = 7.3 Hz, 1H), 4.87 (d, *J* = 15.5 Hz, 1H), 4.47 (d, *J* = 11.4 Hz, 1H), 4.31 (s, 1H), 3.28 (d, *J* = 18.2 Hz, 5H), 2.98 (s, 2H), 2.50 (s, 2H), 2.18 (s, 3H), 1.74 (d, *J* = 25.0 Hz, 2H). ¹³C NMR (101 MHz, DMSO-*d*₆) δ 163.7, 159.6, 158.1, 144.2, 128.2, 127.7, 119.1, 114.8, 110.5, 108.6, 76.5, 66.8, 57.5, 48.5, 45.8, 43.7, 37.1, 27.0, 11.1. HR-MS (ESI): *m/z* [M-H]⁻ calcd for C₁₉H₂₄Cl₂N₇O₃ 468.1323, found 468.1312.

3,4-Dichloro-*N*-((3*S*,4*R*)-3-methoxy-1-(6-(piperazine-1-carbonyl)pyridazin-3-yl)piperidin-4-yl)-5-methyl-1*H*-pyrrole-2-carboxamide (compound **33**). Compound **33** (72 mg, 65%) was prepared from *tert*-butyl piperazine-1-carboxylate (55 mg, 0.28 mmol) in the same manner as described for compound **31** as a white solid. UPLC purity 97.11%. ¹H NMR (500 MHz, chloroform-*d*) δ 7.74–7.68 (m, 1H), 7.27 (d, *J* = 4.7 Hz, 2H), 7.02–6.96 (m, 1H), 5.05 (d, *J* = 15.3 Hz, 1H), 4.33 (d, *J* = 16.0 Hz, 2H), 4.14–4.04 (m, 2H), 3.99–3.88 (m, 2H), 3.55 (s, 1H), 3.42 (d, *J* = 5.3 Hz, 3H), 3.18–3.08 (m, 6H), 2.28 (d, *J* = 5.3 Hz, 3H), 1.97–1.88 (m, 2H). ¹³C NMR (101 MHz, chloroform-*d*) δ 165.2, 159.6, 158.8, 146.7, 129.8, 128.0, 118.4, 111.8, 111.4, 110.5, 76.2, 57.7, 48.9, 43.5, 36.0, 31.9, 27.2, 26.8, 22.7, 14.1, 11.3. HR-MS (ESI): *m/z* [M+H]⁺ calcd for C₂₁H₂₈Cl₂N₇O₃ 496.1625, found 496.1647.

N-((3*S*,4*R*)-1-(6-(Aminomethyl)pyridazin-3-yl)-3-methoxypiperidin-4-yl)-3,4-dichloro-5-methyl-1*H*-pyrrole-2-carboxamide (compound **34**). To a solution of compound **20** (250 mg, 0.61 mmol) in MeOH (4 mL) was added 24% palladium on carbon (60 mg) and acetic acid (0.5 mL). The reaction mixture was stirred for 30 h at room temperature under a hydrogen atmosphere at 0.4 MPa. The reaction mixture was filtered through celite and concentrated under reduced pressure. The crude residue was purified by chromatography (water/acetonitrile = 40%/60%) to afford compound **34** (50 mg, 20%) as a white solid. ¹H NMR (500 MHz, DMSO-*d*₆) δ 7.47 (d, *J* = 9.5 Hz, 1H), 7.40 (d, *J* = 9.5 Hz, 1H), 7.18 (d, *J* = 8.2 Hz, 1H), 4.68 (dt, *J* = 14.8, 2.9 Hz, 1H), 4.43–4.36 (m, 1H), 4.30–4.25 (m, 1H), 4.08 (s, 2H), 3.50 (t, *J* = 2.3 Hz, 1H), 3.28 (s, 3H), 3.24–3.18 (m, 1H), 3.12 (ddd, *J* = 13.9, 10.6, 3.9 Hz, 1H), 2.18 (s, 3H), 1.71 (ddd, *J* = 15.3, 6.8, 3.6 Hz, 2H). ¹³C NMR (126 MHz, DMSO-*d*₆) δ 159.7, 157.6, 147.8, 127.9, 127.3, 118.7, 113.1, 109.7, 108.1, 76.0, 56.8, 48.3, 44.7, 42.5, 42.0, 26.3, 10.6. HR-MS (ESI): *m/z* [M+H]⁺ calcd for C₁₇H₂₃Cl₂N₆O₂ 413.1254, found 413.1246.

N-((3*S*,4*R*)-1-(6-Carbamidoylpyridazin-3-yl)-3-methoxypiperidin-4-yl)-3,4-dichloro-5-methyl-1*H*-pyrrole-2-carboxamide (compound **35**). To a solution of compound **20** (250 mg, 0.61 mmol) in MeOH (6 mL) was added sodium methanol (150 mg, 2.78 mmol) under argon and the reaction mixture was stirred overnight at room temperature. Then ammonium chloride (150 mg, 2.80 mmol) was added to the reaction solution and the mixture

was heated at reflux for about 1 h. After cooling to room temperature, the solvent was removed to give compound **35** (250 mg, 96%) as an orange solid.

UPLC purity 97.75%. ^1H NMR (500 MHz, $\text{DMSO-}d_6$) δ 9.75 (s, 3H), 8.74 (s, 1H), 8.48 (d, $J = 9.8$ Hz, 1H), 7.88 (d, $J = 9.8$ Hz, 1H), 7.57 (d, $J = 8.3$ Hz, 1H), 5.23 (s, 1H), 4.87 (s, 1H), 4.69–4.57 (m, 1H), 3.89 (d, $J = 3.8$ Hz, 1H), 3.67 (d, $J = 14.5$ Hz, 1H), 3.62 (s, 3H), 3.60–3.54 (m, 1H), 2.50 (s, 3H), 2.11 (dq, $J = 11.4, 3.6$ Hz, 1H), 2.02 (qd, $J = 12.5, 12.0, 3.7$ Hz, 1H). ^{13}C NMR (126 MHz, $\text{DMSO-}d_6$) δ 166.9, 161.2, 160.6, 157.7, 138.6, 127.8, 126.5, 118.7, 109.9, 108.1, 76.1, 57.0, 48.1, 42.7, 26.6, 14.1, 10.6. HR-MS (ESI): m/z $[\text{M}+\text{H}]^+$ calcd for $\text{C}_{17}\text{H}_{22}\text{Cl}_2\text{N}_7\text{O}_2$ 426.1207, found 426.1195.

N-(3*S*,4*R*)-1-(6-(2*H*-Tetrazol-5-yl)pyridazin-3-yl)-3-methoxy-piperidin-4-yl)-3,4-dichloro-5-methyl-1*H*-pyrrole-2-carboxamide (compound **36**). To a solution of compound **20** (35 mg, 0.086 mmol) in DMF 2 mL was added sodium azide (6.5 mg, 0.1 mmol) and pyridine hydrochloride (10 mg, 0.086 mmol). The reaction mixture was heated for 8 h at 110 °C until completion determined by TLC, and cooled to room temperature. Then the reaction mixture was slowly poured into 5 mol/L NaOH (2 mL). After stirring for additional 30 min, the mixture was concentrated under reduced pressure, diluted with water, and acidified with 3 mol/L HCl to pH 3. The white precipitate formed was filtered, washed with water and dried to afford compound **36** (17 mg, 45%) as a white solid. UPLC purity 97.75%. ^1H NMR (500 MHz, $\text{DMSO-}d_6$) δ 12.42–12.33 (m, 1H), 7.90 (d, $J = 9.5$ Hz, 1H), 7.43 (d, $J = 9.7$ Hz, 1H), 7.32–7.24 (m, 1H), 4.67 (d, $J = 12.8$ Hz, 1H), 4.40 (d, $J = 12.9$ Hz, 1H), 4.32–4.25 (m, 1H), 3.52 (t, $J = 4.4$ Hz, 1H), 3.39 (d, $J = 9.0$ Hz, 3H), 3.28 (s, 1H), 3.17 (d, $J = 4.8$ Hz, 1H), 2.18 (s, 3H), 2.03–1.93 (m, 1H), 1.80–1.71 (m, 2H). ^{13}C NMR (101 MHz, $\text{DMSO-}d_6$) δ 159.8, 158.1, 128.2, 126.9, 119.1, 113.6, 110.4, 108.6, 76.4, 57.3, 48.7, 45.2, 43.0, 29.5, 29.2, 26.9, 11.1. HR-MS (ESI): m/z $[\text{M}-\text{H}]^-$ calcd for $\text{C}_{17}\text{H}_{18}\text{Cl}_2\text{N}_9\text{O}_2$ 450.0966, found 450.0950.

4.2. Gyrase and topo IV inhibitory assay

Gyrases and Topo IVs of *S. aureus* and *E. coli* bacteria were obtained from Inspiralis Ltd. (Norwich, UK). The gyrases were used at a final concentration of 7.5 nmol/L in a solution of 40 mmol/L HEPES-KOH (pH 7.6), 10 mmol/L magnesium acetate, 10 mmol/L dithiothreitol, 50 g/L BSA, 500 mmol/L potassium glutamate, 1% DMSO, 100 mmol/L ATP, and 10 nmol/L linear pBR322 DNA. Topo IVs were used at a final concentration of 8.5 nmol/L in a solution of 100 mmol/L Tris (pH 7.5), 2 mmol/L magnesium chloride, 1 mmol/L dithiothreitol, 50 g/L BSA, 200 mmol/L potassium glutamate, 1% DMSO, 300 mmol/L ATP, and 10 nmol/L pBR322 DNA. Reactions were conducted in a volume of 10 μL per well. Reactions were initiated with the addition of ATP and mixtures were incubated at 20 °C for 30 min. To quantify ADP concentration, 40 μL of ADP-Glo reagent was added and incubated for 40 min at room temperature after the enzymatic reaction. The luminescence signal was measured using a BioTek Synergy 2 microplate reader. The luminescence data were analyzed using the computer software, Graphpad Prism. Activity (%) was calculated as Eq. (1):

$$\text{Activity (\%)} = [(\text{Lu}-\text{Luc}) / (\text{Lut}-\text{Luc})] \times 100 \quad (1)$$

4.3. Surface plasmon resonance (SPR)

Dilute the GYRB to 50 $\mu\text{g}/\text{mL}$ in immobilization buffer 10 mmol/L sodium acetate, pH 4.0. The activator is prepared by mixing 400 mmol/L EDC and 100 mmol/L NHS (GE) immediately before injection. The CM5 sensor chip is activated for 420 s with the mixture at a flow rate of 10 $\mu\text{L}/\text{min}$ 50 $\mu\text{g}/\text{mL}$ of GYRB in immobilization buffer 10 mmol/L sodium acetate (pH 4.0) is then injected into the Fc4 sample channel for 420 s at a flow rate of 10 $\mu\text{L}/\text{min}$, and typically resulting in immobilization levels of 16,000 RU, the reference channel (Fc3) does not need Ligand Capturing step. The chip is deactivated by 1 mol/L ethanolamine hydrochloride-NaOH (GE) at a flow rate of 10 $\mu\text{L}/\text{min}$ for 420 s. Dilute analytes with the same running buffer to 6 concentrations (400, 200, 100, 50, 25 and 0 nmol/L). The analyte is injected into Fc3–Fc4 of the channel at a flow rate of 20 $\mu\text{L}/\text{min}$ for an association phase of 120 s, followed by 180 s dissociation. The association and dissociation processes are all handled in the running buffer. Repeat 6 cycles of an analyte according to analyte concentrations in ascending order. After each cycle of interaction analysis, the sensor chip surface should be regenerated completely with 10 mmol/L glycine/HCl, pH 1.5 as injection buffer at a flow rate of 30 $\mu\text{L}/\text{min}$ for 30 s to remove the analyte, then next concentration cycle of the analyte demethylzylasteral need to repeat analyte injection and regeneration steps.

4.4. Molecular docking

Redock: At first, the ligand 07N1 (AZD1279 (7)) is docked with the prepared protein by the CDOCKER module of Discovery Studio 2016. (A). Protein preparation: Retain the A chain, ligand (07N1), and HOH2 in the protein, remove heteroatoms and other chains from the protein, clean the protein. Prepare the Protein and Define Site operations on the protein, and cut the ligand to a new window. Save the prepared protein as 3TTZ _ prep _ site _ rec.ds. (B). Ligand preparation: Perform Clean Geometry, Prepare Ligands, and Minimize Ligands operations on the ligand. The prepared ligand is saved as 07N1 _ lig _ rec.sd (C). Docking: CDOCKER the prepared ligands and prepared proteins (D). Results: After docking, the conformations with similar interaction modes and the RMSD value less than 2 were selected.

Dock: (A). Protein Preparation: Use the prepared protein in Redock (B). Ligand (compound **28** and AZD5099 (6)) preparation: Perform Clean Geometry, Prepare Ligands, and Minimize Ligands operations on the molecule to be docked, saving the docked molecule as active _ rec.sd. (C). Docking: CDOCKER the prepared docking molecule and the prepared protein (D). Results: After the docking is completed, a conformation with a similar interaction mode with the ligand is selected.

4.5. Antibacterial assay

The antibacterial activity of all compounds was measured according to the broth dilution method prescribed by the Clinical and Laboratory Standards Institute (CLSI) guidelines. Bacterial cells were cultured overnight at 37 °C 100 μL of each different concentration of the test sample solution was added to the sterilized 96-well polystyrene plate, and the final concentrations of the drug were 128, 64, 32, 16, 8, 4, 2, 1, 0.5, 0.25, 0.125, 0.06, 0.03, 0.015, 0.008 $\mu\text{g}/\text{mL}$,

respectively. 100 μL of the bacterial suspension was added to each well (200 μL per well), and the final concentration of the solution was about 10^5 CFU/mL. The plates were sealed and incubated in an incubator at 35–37 $^{\circ}\text{C}$ for 18–24 h to determine the results. The lowest drug concentration that completely inhibits the growth of bacteria is the Minimal Inhibitory Concentration (MIC). All tests were performed at least twice with biological replicates.

4.6. Killing kinetic studies

The killing kinetic assay on *S. aureus* (ATCC 29213) was performed in 96-well plates on DS2969 (**5**), compound **28** at four different concentrations (1 \times MIC, 4 \times MIC, 8 \times MIC, 16 \times MIC), and the concentration of the bacterial solution in each well was 10^5 CFU/mL. The microplates were incubated at 37 $^{\circ}\text{C}$. The viable cell count was assessed at 0, 1, 2, 4, 8 and 24 h.

4.7. Spontaneous drug resistance frequency

S. aureus (ATCC43300 and ATCC29213) were incubated in Mueller-Hinton (MH) broth overnight at 37 $^{\circ}\text{C}$. The bacteria were collected by centrifugation at 3000 r/min, and the supernatant was removed and the concentration of the bacteria was adjusted to 10^{10} CFU/mL with sterile physiological saline. The above solution (100 μL) was applied to MH agar dishes containing drugs at the concentration of 4 \times MIC, incubated at 37 $^{\circ}\text{C}$ for 48 h, and the number of colonies on the plates was recorded.

4.8. Mitochondrial toxicity

The protocol was reported by Cotman and coworkers³⁰. HepG2 cells (50,000) were seeded in each well of two 96-well plates, and 100 μL of growth medium (glucose media) was added. Cells were allowed to adhere overnight in a cell incubator at 37 $^{\circ}\text{C}$. The next day, the medium was removed, cells were washed with PBS, and 100 μL of medium (with glucose) containing positive control (Rotenone) was added, before the addition of the test compounds. The same procedure was repeated for plate 2 with medium replaced with galactose. Cells were again incubated at 37 $^{\circ}\text{C}$ for 24 h. CellTiter-Glo 2.0 Cell Viability (100 μL) (Promega) was then added to each well to measure the amount of ATP. The plate was placed in a shaker for 2 min and incubated for 15 min in the dark at 22 $^{\circ}\text{C}$. Luminescence was read in a luminometer Tecan Infinite 200 pro. Luminescence from each well treated with the compound was compared to the negative control (medium only).

4.9. Cytotoxicity assay

The selected cells were cultured in RPMI1640 medium supplemented with 10% fetal bovine serum (FBS). The cells were incubated in a humidified atmosphere of 5% CO_2 at 37 $^{\circ}\text{C}$. Stocks of cells were cultured in 25 cm^2 tissue culture flasks and subcultured two to three times per week. Cytotoxicity testing was performed in a transparent 96-well microplate. Outer perimeter wells were filled with sterile water to prevent dehydration in experimental wells. The cells were

incubated at 37 $^{\circ}\text{C}$ under 5% CO_2 until confluent and then diluted with culture medium to 4×10^5 cells/mL. Dilutions of the stock solutions resulted in final concentrations of 10 $\mu\text{g}/\text{mL}$ in a final volume of 100 μL . After incubation at 37 $^{\circ}\text{C}$ for 48 h, the medium was removed, and the monolayers were washed twice with 100 μL of warm Hanks' balanced salt solution (HBSS). Warm medium (100 μL) and 10 μL of freshly made methylthiazolyldiphenyltetrazolium bromide (MTT) were added to each well, and then the plates were incubated for 4 h. The absorbance was determined at 570 nm.

4.10. Inhibition evaluation on hERG K^+ channel

HEK293 cells were stably transfected with the human ether-a-go-go-related gene (hERG channel). The voltage-gated hERG potassium channel current was recorded at room temperature (25 $^{\circ}\text{C}$) from randomly selected transfected cells under whole-cell manual patch clamp systems equipped with EPC10 amplifier (HEKA, Germany), while electrical data were digitalized by Digidata1440A with sampling frequency at 10 kHz using Patchmaster v2.0. hERG current inhibition at 10 and 30 $\mu\text{mol}/\text{L}$ was tested. Quinine was also included as a positive control to ensure the accuracy and sensitivity of the test system.

4.11. Animal experimental protocols

The animal experimental protocols were conducted in accordance with the principles of the NIH Guide for the Care and Use of

$$\text{Spontaneous resistance frequency} = \frac{\text{The number of colonies on the plate}}{\text{The actual inoculum CFU of the plate}} \quad (2)$$

Laboratory Animals and approved by the Institutional Animal Care and Use Committee of the Institute of Material medica, Chinese Academy of Medical Sciences. The male ICR mice (20–22 g) were obtained from Beijing Vital River Laboratory Animal Technology Co., Ltd. The beagle dogs (10–12 kg) were obtained from Beijing Mars Biotechnology Co., Ltd.

4.12. Mouse model of sepsis

ICR mice (2 males and 2 females/group) were intraperitoneal injection with a minimum lethal dose ($\sim 10^8$ CFU) of *S. aureus* strain (ATCC 43300). After 1 h, the compounds **14**, **22**, **23**, **28**, DS2969 (**5**), and AZD5099 (**6**) were administered by intragastric administration (ig) at a dose of 10 mg/kg. The survival of animals was recorded daily for 7 days.

4.13. Neutropenic murine thigh *S. aureus* infection models

The ICR mice were rendered neutropenic by twice intraperitoneal injections of cyclophamide for and on the 1st day and 4th day (150 and 100 mg/kg). After the *S. aureus* strain (ATCC43300, 10^6 CFU) was injected into the thigh muscles on the 5th day, compound **28** was administered by tail vein injection at doses of 0.05, 0.5, and 2.5 mg/kg respectively. At the end of 24 h, the animals were sacrificed, and their thigh muscles were removed and homogenized in the iced sterile physiological saline. The CFU of *S. aureus* was evaluated by serial dilutions.

4.14. Mouse acute toxicity test

ICR mice were divided into blank, intragastric administration (200, 300, 600, 800 mg/kg), intraperitoneal injection (200, 300, 600 mg/kg), and tail vein injection (25, 50, 100, 150 mg/kg) group with different dosage (2 males and 2 females/group). After the single-dose administration of compound **28**, the survival of animals was recorded daily for 7 days.

4.15. Mouse subacute toxicity test

ICR mice were divided into blank, low-dose groups (150 mg/kg) and high-dose groups (300 mg/kg) (5 males and 5 females/group). After the repeated gavage administrations of compound **28** for one week (7 days), the mice were euthanized and the main organ tissues (heart, liver, spleen, lungs, kidneys, adrenal glands, thyroid gland, uterus, ovaries, brain, bladder, gallbladder, etc.) were separated and observed.

4.16. Pharmacokinetics study on the beagle dogs

The beagle dogs were fasted for 12 h before the experiment. The pharmacokinetics study of compound **28** in beagle dogs (5 males and 5 females) after oral administration and fore limb intravenous injection at the dose of 1 mg/kg. The blood samples were collected at 0.08, 0.17, 0.25, 0.50, 0.75, 1, 2, 3, 5, 6, 8, 10, 12, 24, 36, and 48 h after the administration of compound **28**. The concentrations in plasma were determined using LC–MS/MS. The pharmacokinetic data were analyzed.

Acknowledgments

The authors thank the financial support from the CAMS Innovation Fund for Medical Sciences (2021-I2M-1-030, China) and the Science and Technology Commission Foundation of Beijing (Z221100007922045, China).

Author contributions

Wenxuan Zhang and Song Wu: conceptualization, methodology, supervision, writing reviewing, and editing. Xintong Zhao, Jing Feng, Jie Zhang: methodology, investigation, acquisition of data, writing-original draft. Zunsheng Han, Yuhua Hu, Hui–Hui Shao, Tianlei Li, Jie Xia, Kangfan Lei, Weiping Wang, Fangfang Lai, Yuan Lin, Bo Liu, Kun Zhang, Chi Zhang, Qingyun Yang, Xinyu Luo, Hanyilan Zhang, Chuang Li: investigation, acquisition of data, technical or material support. The manuscript was written through the contributions of all authors. All authors have approved the final version of the manuscript.

Conflicts of interest

The authors declare no competing interests.

Appendix A. Supporting information

Supporting data to this article can be found online at <https://doi.org/10.1016/j.apsb.2023.08.030>.

References

- O'Neill J. Antimicrobial Resistance: Tackling a crisis for the health and wealth of nations. *Review on Antimicrobial Resistance* 2014. Available from: https://amr-review.org/sites/default/files/AMR_Review_Paper_-_Tackling_a_crisis_for_the_health_and_wealth_of_nations_1.pdf.
- Murray CJL, Ikuta KS, Sharara F, Swetschinski L, Aguilar GR, Gray A, et al. Global burden of bacterial antimicrobial resistance in 2019: a systematic analysis. *Lancet* 2022;**399**:629–55.
- Miethke M, Pieroni M, Weber T, Brönstrup M, Hammann P, Halby L, et al. Towards the sustainable discovery and development of new antibiotics. *Nat Rev Chem* 2021;**5**:726–49.
- Hutchings MI, Truman AW, Wilkinson B. Antibiotics: past, present and future. *Curr Opin Microbiol* 2019;**51**:72–80.
- Chang CC, Wang YR, Chen SF, Wu CC, Chan NL. New insights into DNA-binding by type IIA topoisomerases. *Curr Opin Struct Biol* 2013;**23**:125–33.
- Yi L, Lu X. New Strategy on antimicrobial-resistance: inhibitors of DNA replication enzymes. *Curr Med Chem* 2019;**26**:1761–87.
- Tomb JF, White O, Kerlavage AR, Clayton RA, Sutton GG, Fleischmann RD, et al. The complete genome sequence of the gastric pathogen *Helicobacter pylori*. *Nature* 1997;**388**:539–47.
- Schmutz E, Mühlenweg A, Li SM, Heide L. Resistance genes of aminocoumarin producers: two type II topoisomerase genes confer resistance against coumermycin A1 and clorobiocin. *Antimicrob Agents Chemother* 2003;**47**:869–77.
- Gellert M, Mizuuchi K, O'dea MH, Nash HA. DNA gyrase: an enzyme that introduces superhelical turns into DNA. *Proc Natl Acad Sci U S A* 1976;**73**:3872–6.
- Sissi C, Palumbo M. In front of and behind the replication fork: bacterial type IIA topoisomerases. *Cell Mol Life Sci* 2010;**67**:2001–24.
- Dighe SN, Collet TA. Recent advances in DNA gyrase-targeted antimicrobial agents. *Eur J Med Chem* 2020;**199**:112326.
- Azam MA, Thathan J, Jubie S. Dual targeting DNA gyrase B (GyrB) and topoisomerase IV (ParE) inhibitors: a review. *Bioorg Chem* 2015;**62**:41–63.
- Pham TDM, Ziora ZM, Blaskovich MAT. Quinolone antibiotics. *Medchemcomm* 2019;**10**:1719–39.
- Bush NG, Diez-Santos I, Abbott LR, Maxwell A. Quinolones: mechanism, lethality and their contributions to antibiotic resistance. *Molecules* 2020;**25**:5662.
- Fairbrother RW, Williams BL. Two new antibiotics: antibacterial activity of novobiocin and vancomycin. *Lancet* 1956;**268**:1177–9.
- Price KE, Chisholm DR, Leitner F, Misiek M. Microbiological and pharmacological evaluation of BL-C43, a new semisynthetic derivative of coumermycin A1. *Antimicrob Agents Chemother* 1969;**9**:209–18.
- Lewis RJ, Singh OM, Smith CV, Skarzynski T, Maxwell A, Wonacott AJ, et al. The nature of inhibition of DNA gyrase by the coumarins and the cyclothialidines was revealed by X-ray crystallography. *EMBO J* 1996;**15**:1412–20.
- Bisacchi GS, Manchester JL. A new-class antibacterial-almost. lessons in drug discovery and development: a critical analysis of more than 50 years of effort toward ATPase inhibitors of DNA gyrase and topoisomerase IV. *ACS Infect Dis* 2015;**1**:4–41.
- Barancokov M, Kikelj D, Ilaš J. Recent progress in the discovery and development of DNA gyrase B inhibitors. *Future Med Chem* 2018;**10**:1207–27.
- Durcik M, Tomašič T, Zidar N, Zega A, Kikelj D, Mašič LP, et al. ATP-competitive DNA gyrase and topoisomerase IV inhibitors as antibacterial agents. *Expert Opin Ther Pat* 2019;**29**:171–80.
- Jaswal S, Nehra B, Kumar S, Monga V. Recent advancements in the medicinal chemistry of bacterial type II topoisomerase inhibitors. *Bioorg Chem* 2020;**104**:104266.
- Man RJ, Zhang XP, Yang YS, Jiang AQ, Zhu HL. Recent progress in small molecular inhibitors of DNA Gyrase. *Curr Med Chem* 2021;**28**:5808–30.

23. Talley AK, Thurston A, Moore G, Gupta VK, Satterfield M, Manyak E, et al. First-in-human evaluation of the safety, tolerability, and pharmacokinetics of SPR720, a novel oral bacterial DNA gyrase (GyrB) inhibitor for mycobacterial infections. *Antimicrob Agents Chemother* 2021;**65**:01208–21.
24. Locher CP, Jones SM, Hanzelka BL, Perola E, Shoen CM, Cynamon MH, et al. A novel inhibitor of gyrase B is a potent drug candidate for treatment of tuberculosis and nontuberculosis mycobacterial infections. *Antimicrob Agents Chemother* 2015;**59**:1455–65.
25. Vandell AG, Inoue S, Dennie J, Nagasawa Y, Gajee R, Pav J, et al. Phase I study to assess the safety, tolerability, pharmacokinetics, and pharmacodynamics of multiple oral doses of DS-2969b, a novel GyrB inhibitor, in healthy subjects. *Antimicrob Agents Chemother* 2018;**62**:02537. 17.
26. Basarab GS, Hill PJ, Garner CE, Hull K, Green O, Sherer BA, et al. Optimization of pyrrolamide topoisomerase II inhibitors toward identification of an antibacterial clinical candidate (AZD5099). *J Med Chem* 2014;**57**:6060–82.
27. Sherer BA, Hull K, Green O, Basarab G, Hauck S, Hill P, et al. Pyrrolamide DNA gyrase inhibitors: optimization of antibacterial activity and efficacy. *Bioorg Med Chem Lett* 2011;**21**:7416–20.
28. Phillips J, Goetz M, Smith S, Zink D, Polishook J, Onishi R, et al. Discovery of kibdelomycin, a potent new class of bacterial Type II topoisomerase inhibitor by chemical-genetic profiling in *Staphylococcus aureus*. *Chem Biol* 2011;**18**:955–65.
29. Durcik M, Nyerges Á, Ž Skok, Skledar DG, Trontelj J, Zidar N, et al. New dual ATP-competitive inhibitors of bacterial DNA gyrase and topoisomerase IV active against ESKAPE pathogens. *Eur J Med Chem* 2021;**213**:113200.
30. Cotman AE, Durcik M, Tiz DB, Fulgheri F, Secci D, Sterle M, et al. Discovery and hit-to-lead optimization of benzothiazole scaffold based DNA gyrase inhibitors with potent activity against *Acinetobacter baumannii* and *Pseudomonas aeruginosa*. *J Med Chem* 2023;**66**:1380–425.
31. Fink MP. Animal models of sepsis. *Virulence* 2014;**5**:143–53.
32. Andes DR, Lepak AJ. *In vivo* infection models in the pre-clinical pharmacokinetic/pharmacodynamic evaluation of antimicrobial agents. *Curr Opin Pharmacol* 2017;**36**:94–9.
33. Bassetti M, Garau J. Current and future perspectives in the treatment of multidrug-resistant Gram-negative infections. *J Antimicrob Chemother* 2021;**76**:iv23–37.
34. Richter MF, Drown BS, Riley AP, Garcia A, Shirai T, Svec RL, et al. Predictive compound accumulation rules yield a broad-spectrum antibiotic. *Nature* 2017;**545**:299–304.